MAY 7 1946

Registered No. M 3121

PROCEEDINGS

OF THE

INDIAN ACADEMY OF SCIENCES

VOL. XXIII] *SECTION A* [No. 2

FEBRUARY, 1946

Price Rs. 2 or 3 Sh. *Annual Subscription Rs. 18*

PRINTED AT THE BANGALORE PRESS, BANGALORE CITY, BY G. SRINIVASA RAO, SUPERINTENDENT, AND PUBLISHED BY THE INDIAN ACADEMY OF SCIENCES, BANGALORE.

EXPERIMENTS ON THE RADIAL VARIATION OF CRITICAL VELOCITY OF WATER IN TUBES OF CIRCULAR CROSS-SECTION

By Major D. L. Deshpande, F.A.Sc., M.Sc. (Manch.), M.I.E., A.M.I. Mech. E.

(Principal, College of Engineering, Trivandrum)

Received October 13, 1945

The present investigation was planned with a view of determining, if possible, at what point in the cross-section of a parallel tube through which water flows with stream-line motion, this motion first breaks down and becomes turbulent as the velocity is increased.

It was thought that this information might be of value as possibly affording some indication of the reason for the change from stream-line to turbulent motion at the critical velocity.

The Apparatus

The apparatus used in the tests was a modification of that on which Osborne Reynolds carried out his classical experiments on critical velocities. It consists of a large glass-sided tank 5–10½″ long by 18″ wide, fitted with baffles for steadying the flow from the inlet pipe, from which water was allowed to flow through a glass tube. The rate of flow was regulated by a valve at the outlet from the tube. The inlet end of the tube was fitted with a carefully finished bell mouthpiece.

The motion in the tube was made visible by a colour band of aniline dye, supplied from a tank and discharged through a fine capillary tube at the entrance to the bell mouthpiece. The position of this capillary tube could be regulated with precision both in a horizontal and a vertical direction by means of adjusting screens on its carrier.

At the point of observation of the coloured filament, the tube was enclosed in a glass-sided box, having vertical sides of parallel plate glass. The box had an open top and was filled with water.

In order to obtain the distance of the filament from the centre of the tube, a graduated scale was mounted on the vertical glass front of the box surrounding the tube, and a similar scale in the same plane across the open top of the box.

Above the box a plane mirror was mounted at 45° to the horizontal.

For observing the filament, two telescopes were mounted horizontally, one above the other, in the same vertical plane, *i.e.*, the plane containing the graduated scales. The upper one was focussed on the scale and on the filament, which was observed from above through the mirror, while the lower one was focussed on the filament as seen through the side of the box.

In this way the position of the filament at the section in question, with reference to each of the scales, and therefore with reference to the axis of the tube was obtained.

In order to correct for refraction, a thin graduated scale was made to fit the internal diameter of the tube. This was inserted into the tube, which was filled with water as when carrying out an experiment, and the readings of the internal and external scales were compared over the whole radius. The experiments were carried out on tubes of four diameters, *viz.*, 0·5″; 1·0″; 1·25″; and 1·5″.

Method of Carrying out Experiments

In carrying out an experiment the supply tank was filled and allowed to stand for some time in order to allow any initial disturbance of the water to die out. Some definite cross-section of the tube, at which to take observations, was then selected and the telescopes and gauges were brought into this plane. The outlet valve was then slightly opened and the rate of flow of the dye was regulated so as to give a fine colour band.

The opening of the outlet valve was then gradually increased until a slight flicker of the colour band was noticed near the outlet end of the tube. This indicates that the velocity was approaching the critical value.

A very slight increase in the velocity caused definite but intermittent breakdown into eddy formation at the end of the tube. A further slight increase in the velocity caused the eddies to become permanent and brought the point of breakdown nearer to the tube entrance. In this way by adjusting the velocity the point of breakdown with the filament at any required radius, could be brought into the plane of observation.

The exact radial position of the filament at this section was then observed and recorded, after which the mean velocity in the tube was determined by observing the time for the level in the supply tank to fall through a given distance when discharging under the same head with the inlet valve closed. The inverse of this time was proportional to the mean velocity of flow. With

each tube the experiments were carried out for a series of radial positions of the filament, extending from the centre to a point near the walls.

Experimental Data

(1) *Experiments on tube* 1·5″ *diameter.*—This tube was 5·0′ long and the observations were made at a point distant 2·0 ft. from the inlet end.

The co-ordinates of the centre of the tube on the horizontal and vertical scale were:

Horizontal scale	..	..	.. 4·38″
Vertical ,,	..	..	.. 1·32″

The following table, which represents a typical set of observations, shows the horizontal and vertical co-ordinates of the filament at the instant of break-down; its radial distance from the centre of the tube; and the corresponding time for the level in the supply tank to fall through a distance of 1 inch.

Position of Colour Band		Distance from Centre	Time (Secs.) for Level in Tank to fall 1·0″
Horizontal	Vertical		
4·38	1·33	·01	42·5
4·30	1·38	·1	44·0
4·25	1·32	·230	48·2
4·15	1·49	·285	51·2
4·24	1·06	·295	52·2
4·63	1·04	·38	58·5
3·00	1·34	·38	58·0
4·00	1·35	·39	59·1
4·11	1·65	·427	62·2
4·50	0·90	·438	63·0
4·51	0·90	·44	63·2
4·00	1·10	·44	63·2
3·96	1·16	·45	64·0
4·81	1·40	·50	66·0
4·02	1·70	·53	62·8
3·88	1·52	·538	62·5
4·45	1·84	·556	59·8
4·07	1·73	·515	66·0
3·80	1·32	·58	55·5
3·90	1·00	·583	56·0
4·05	1·82	·60	49·9
4·85	0·95	·632	45·0
4·01	1·83	·632	45·0

These times are plotted on a base showing the distance from the centre of the tube of the corresponding filament. From this it will be seen that as the distance of the filament from the centre of the tube increases, the velocity of flow necessary to produce break-down into turbulent motion

diminishes and attains a minimum value at a radius of approximately 0·5″ after which it increases with a further increase in radius.

This indicates that when, owing to increasing the velocity motion is made to break down at this section, the breakdown first occurs at a radius of approximately 0·475, or at a distance from the centre equal to 0·63 of the radius of the tube.

(2) *Experiments on tube* 1·25″ *diameter.*—This tube was 4·33′ long and the observations were made at a point distant 2·5′ from the inlet end.

The co-ordinates of the centre of the tube were:

Horizontal scale .. .. .. 2·48″

Vertical „ .. .. .. 4·87″

The following table shows a set of experimental observations on the tube.

Position of Colour Band		Distance from Centre inches	Time from 12″ to 11″ (Secs.)
Horiz. Scale	Vert. Scale		
2·49	4·91	·04	62·8
2·47	4·80	·07	64·2
2·50	4·78	·092	55·6
2·60	4·71	·20	57·0
2·50	4·62	·25	61·2
2·48	4·62	·25	60·2
2·49	4·56	·31	75·0
2·49	4·51	·36	87·2
2·47	4·48	·39	86·2
2·49	4·44	·43	79·0
2·49	4·42	·45	72·5
2·50	4·40	·47	62·6
2·48	4·30	·57	75·0

As in the tests on the 1·5″ tube, the velocity necessary to cause breakdown at this section diminishes with the distance of the filament from the centre of the tube and attains a minimum at a radius of 0·37″ or 0·595 of the radius of the tube; afterwards increasing as the radius of the filament is increased.

(3) *Experiments on tube* 1·0″ *diameter.*—In order, if possible, to ensure that the position of the radius at which breakdown first occurs should not be affected by the stabilising effect of the bell-mouthed entrance to the tube, a larger tube—10′ in length—was obtained for the second series of experiments. This tube was 1·0″ in diameter, and the observations were made at a section distant 5·0′ or sixty pipe diameters from the inlet.

The co-ordinates of the centre of this tube were:

Horizontal scale .. .. .. 4·08″
Vertical „ .. .. .. 1·66″

The following table shows a typical set of experimental observations on this tube.

Experiments on 1″ *tube, Length* 10′

Co-ordinates of Centre (1.66 : 4.08)

Position of Colour Band		Distance from Centre	Time (Secs.) for Level in Tank to fall 1·0″
Vertical	Horizontal		
1·66	4·08	·0	75·6
1·73	4·10	·071	79·0
1·56	4·08	·10	80·1
1·59	4·00	·106	82·3
1·70	3·94	·146	86·1
1·60	3·89	·199	90·3
1·73	3·88	·212	100·8
1·70	3·80	·282	108·1
1·70	3·75	·331	112·7
1·90	3·77	·388	108·0
1·68	3·69	·395	90·7
1·63	3·68	·410	81·5

It will be seen that, as in the tests on the 1·5″ tube, the velocity necessary to cause breakdown at this section diminishes with the distance of the filament from the centre of the tube, and attains a minimum at a point whose radius (0·33″) is 0·66 of the radius of the tube, afterwards increasing with an increase in the radius.

(4) *Experiments on tube* 0·5″ *diameter.*—This tube was 7·0′ long, and observations were made in this case at three sections; Section A was at a distance of 19″ from the entrance; Section B, 43″ from the entrance; and Section C, 72″ from the entrance.

The experimental data are shown in the following tables.

On comparing these, it appears that the radius of the tube at which the minimum velocity is required to cause breakdown is sensibly the same in each case, namely, 0·165″ or 0·66 of the radius of the tube.

The mean velocities required to cause this breakdown, however, diminish very appreciably with the distance from the entrance. If the velocity required to breakdown at Section C be taken as unity, that at Section B is 1·17, and that at Section A is 1·91.

SECTION A

Distance 1'–7" from entrance

Centre co-ordinates (3·87 : 1·02)

Position of Colour Band		Distance from Centre	Time (Secs.) for Level in Tank to fall 1·0"
Horizontal	Vertical		
3·87	1·025	·005	60·1
3·88	1·02	·01	64·0
3·87	1·03	·01	63·6
3·87	1·07	·05	69·0
3·81	1·02	·06	71·0
3·95	1·03	·081	78·0
4·00	1·02	·13	96·0
3·87	1·165	·145	103·5
4·01	1·09	·16	107·0
4·01	1·10	·166	109·4
3·88	1·20	·180	75·
3·74	1·16	·189	94·1
4·09	1·02	·22	75·1
4·07	1·16	·248	65·0

SECTION B

Centre co-ordinates (3·875 : 0·935)

Position of Colour Band		Distance from Centre	Time (Secs.) for Level in Tank to fall 1·0"
Horizontal	Vertical		
3·87	·96	·030	157·9
3·91	·93	·04	153·5
3·90	·90	·042	161·1
3·94	·93	·070	159·0
3·90	1·00	·076	153·8
3·84	1·04	·114	171·2
3·99	·93	·120	159·0
3·91	·80	·136	177·0
4·02	·93	·150	178·5
3·93	·78	·158	179·1
4·00	·83	·164	180·8
4·05	·84	·175	179·4
4·03	1·03	·186	173·5
4·04	·83	·197	168·5
4·08	·950	·212	161·1
4·08	·860	·22	157·5
4·08	·860	·22	155·0

This is due to the stabilising effect of the bell-mouth entrance, which is evidently still slightly felt at Section B which is 86 tube diameters from the entrance.

SECTION C

Taken at 6′ from entrance

Centre co-ordinates (3·89 : ·92)

Poaition of Colour Band		Distance from Centre	Time (Secs.) for Level in Tank to fall 1·0″
Horizontol	Vertical		
3·90	·92	·01	194·5
3·90	·933	·016	195·8
3·91	·933	·024	196·1
3·89	·95	·03	194·0
3·89	1·00	·18	196·0
3·89	1·02	·10	198·1
3·99	1·00	·127	202·5
3·89	1·06	·140	200·8
3·99	1·05	·15	205·1
4·04	·99	·158	208·3
4·02	1·01	·166	210·3
4·01	1·06	·189	206·3
4·19	·92	·20	200·1

Careful measurements of the diameter of this 0·5″ tube showed that it varies slightly, to the extent of 0·06″ in its length of 7′. The experiments already described had been carried out with the smaller end at the entrance, and in order to determine the effect of this, the tube was reversed and the experiment repeated, observations being made at a point (Section D) corresponding to Section C, *i.e.*, 72 ins. from the entrance.

The results of this experiment are shown in the following table.

SECTION D

(*Tube reversed*)

Taken at 6′ from the entrance end

Centre co-ordinates (3·86 : ·975)

Position of Colour Band		Distance from Centre	Time (Secs.) for Level in Tank to fall 1·0″
Horizontal	Vertical		
0·97	3·86	·005	121·1
1·00	3·89	·042	122·3
0·94	3·90	·050	122·9
0·90	3·90	·080	125·0
0·97	3·95	·090	127·3
1·03	3·93	·093	127·9
1·10	3·83	·133	136·1
1·03	3·98	·136	137·0
1·05	3·98	·144	137·8
1·12	3·86	·150	138·0
1·05	4·00	·161	139·1
1·13	3·92	·172	139·0
1·14	3·99	·214	133·1

The results show that while the radius of maximum instability is at the same point as before (at 0·66 of the radius of the tube) the velocity necessary to cause breakdown at this radius is 1·5 times as great as with flow in the opposite direction.

Ratio of Velocities Required to Cause Breakdown of Motion at Centre and at Radius of Maximum Instability

From the various graphs, the ratio of the velocities required to cause breakdown of the motion at the radius of maximum instability and at the centre, can be obtained. These are as follows:

		Diam of tube "	Ratio
		1·5	0·65
		1·25	0·65
		1·0	0·70
		0·5	..
Slightly divergent ..	19" from entrance ..	..	0·56
	43 " " ..	..	0·88
	72 " " ..	..	0·92
Slightly convergent ..	72 " " ..	..	0·88

These figures show that this ratio is greatly affected by the proximity to the bell-mouthpiece. On the whole, it would appear that the ratio increases slightly as the pipe diameter is decreased.

Critical Velocity near the Wall of a Tube

In the experiments an observation very near the wall of the tube was found to be very difficult. If the tube supplying the colour band was so adjusted that the colour band was very near the wall, it almost invariably touched the wall before observations could be made, and remained in contact with the wall.

If, however, the curves be produced to a radius corresponding to that of the respective tubes, it appears that the velocity required to produce breakdown of motion near the wall is much greater than that required at any other point in the cross-section. Taking the curves as a whole, it appears that the critical velocity is the same as at the centre, at a point whose radius is approximately 0·85 of the radius of the tube.

Conclusions and Deductions

All the experiments indicate that when breakdown of motion initially streamline into turbulent motion occurs during flow through a tube, the

breakdown first occurs at a distance from the centre of the pipe, the experimental values ranging from 0·60 to 0·67 in the different tubes. From this point the turbulence spread inwards to the centre and outwards to the walls.

The exact reason for the breakdown or the mechanism producing it is not as yet understood. It is known to be due to the presence of the pipe walls, and to be independent of the roughness of the walls so long as the roughness is small. It is not due to the attainment of a limiting shear stress in the fluid, since stream-line motion is possible in a small tube with shear stresses much greater than that obtaining at the critical velocity in a larger tube.

An examination of the problem in the light of the experimental data of the present investigation, suggests that the breakdown may be related to the rate of variation of energy across a diameter of the tube. Since the pressure across a section of a parallel tube in which the flow is stream-line is constant, the rate of variation of the energy per unit mass along a radius is the same as the rate of change of the kinetic energy and therefore of v^2.

Assuming that some slight deviation of the particles from linear axial flow to be produced in any way, this will have its maximum disturbing effect it if occurs at a radius where the radial rate of change of energy is a maximum and therefore where $\frac{dv^2}{dr}$ is a maximum.

But in stream-line flow through a tube of radius a,

$$v \propto (a^2 - r^2)$$

$$\therefore \quad \frac{dv^2}{dr} \propto (a^2 - r^2)\, r,$$

which is a maximum when $r = \frac{a}{\sqrt{3}} = 0{\cdot}58\, a$.

It is suggestive that this is very nearly the radius at which breakdown occurred in the experiments. The fact that the experimental value is somewhat greater than this is possibly due to the fact that in a tube whose walls are not perfectly smooth, those filaments nearest the walls suffer some slight lateral displacement due to the roughness, and thereby suffer a reduction in stability causing breakdown to occur somewhat nearer the walls than would be the case in an ideally smooth tube. That this is a possible explanation is indicated by the fact that the radius of primary breakdown in the experiments was smallest in the two larger tubes, having a mean value of $0{\cdot}615\, a$ in these tubes, as compared with $0{\cdot}66\, a$ in the smaller tubes. As the surface

finish of all the tubes was as nearly as could be determined the same, the relative roughness would be smaller in the larger tubes.

It is to be noted that at the radius $(a/\sqrt{3})$, the value of $\frac{dv^2}{dr}$ is proportional to $a^2 \frac{dp}{dl}$ where $\frac{dp}{dl}$ is the pressure drop per unit length of the tube.

But in the similar tubes the product $a\bar{v}$, where $\bar{v}$ is the mean velocity, is constant at the critical velocity, while $\frac{dp}{dl} \propto \frac{\bar{v}}{a^2}$ $\therefore a^2 \frac{dp}{dl}$ or $\frac{dv^2}{dr}$ is a constant at the critical velocity in tubes of different diameter.

From this it would appear that in any tube the breakdown from streamline to turbulent motion, occurs when the gradient of energy along the radius exceeds a certain definite value, and that this factor is the criterion of such a breakdown.

EFFECT OF SURFACE-ACTIVE AGENTS ON INDICATORS†

By T. Krishnappa, K. S. Gururaja Doss* and B. Sanjiva Rao‡

Received October 31, 1945

Introduction

It is known that surface-active substances influence the determination of pH when carried out by the indicator method. Smith and Jones[1] found that the presence of commercial wetting agents (Gardinol CA and Gardinol WA) often caused an error of more than one unit in pH when the common indicators are employed in the measurement. Hartley[2] made an extensive qualitative study of the phenomenon employing paraffin chain salts and found that the order of magnitude of the influence could be correlated with the valence change in indicators accompanying the colour change. In a recent paper, Hartley and Roe[3] have attempted to correlate the observed displacement of pH with the cataphoretic mobility of the micelles of the paraffin chain salts. The object of the present work is to study the effect quantitatively with a view to elucidate the phenomenon.

Experimental

The surface active substances used in the present work are Nekal BX (sodium di-alkyl naphthalene sulphonate) and Igepon T (sodium salt of oleyl-N-methyltaurine). Nekal BX was purified by the method described previouly.[4] Igepon T was purified by a similar method using ethyl alcohol as the solvent. The product was dried in vacuum at 80° C. to 90° C. as it melted when dried at 100° C.

The indicators employed were thymol blue and bromphenol blue supplied by the Hellige Company along with their comparator. 0·04 per cent. solutions were prepared by dissolving the solid indicators in the requisite quantity of alkali and making up with water.[5]

The Hellige comparator was found to be unsuitable for the present work. Apart from the method being approximate (correct only to 0·2 unit) it was found impossible to match the colour of the test solution against any of the

† Part of Thesis submitted by T. K. in partial fulfilment of the requirements for the degree of Master of Science in the University of Mysore.

* Physical Chemist, Imperial Institute of Sugar Technology, Cawnpore.

‡ Head of the Department of Chemistry, Central College, Bangalore.

discs, when the wetting agent was present. For, the wetting agent is found to influence the light absorption characteristics of the indicators. The Hellige colorimeter was therefore employed for determining the ratio of the concentration of basic form to that of the acid form present in the test solution. The apparent pH was calculated therefrom by means of the equation $pH = pK + \log \frac{(\text{basic form})}{(\text{acid form})}$. The standards used for such comparison always contained the wetting agent in the same concentration as in the test solution thus compensating for the change in the absorption characteristics. By taking this precaution excellent matching could always be obtained. With bromphenol blue colour matching was not so good. The standards used were of the following composition:—

Standards for thymol blue—

Acid standard.—The solution was made up from:

(*a*) 0·5 c.c. of the stock solution of the indicator.
(*b*) 1·0 c.c. of 2 N hydrochloric acid solution.
(*c*) Wetting agent in quantities to give the same concentration as in test solution. And
(*d*) Water to make up to 10 c.c.

Basic standard :—

(*a*) 0·5 c.c. of the stock solution of the indicator.
(*b*) Acetate buffer of pH 4·7 having sodium acetate concentration 0·2 N.
(*c*) Sufficient amount of wetting agent to give the same concentration as in test solution. And
(*a*) Water to make up to 10 c.c.

Standards for bromphenol blue—

Acid standard:—

(*a*) 0·5 c.c. of the stock solution of the indicator.
(*b*) 1 c.c. of 2 N hydrochloric acid solution.
(*c*) Wetting agent in quantities to give the same concentration as in the test solution. And
(*d*) Water to make up to 10 c.c.

Basic standard :—

(*a*) 0·5 c.c. of the stock solution of the indicator.
(*b*) 5 c.c. of N sodium acetate.
(*c*) Wetting agent in quantities to give the same concentration as in the test solution. And
(*d*) Water to make up to 10 c.c.

Test solutions were prepared as follows:—

(*a*) 0·5 c.c. of the stock solution of the indicator.

(*b*) Sodium acetate and hydrochloric acid in quantities to give a pH in the working range of the indicator and ionic strength of either 0·1 or 0·01 as required.

(*c*) Wetting agent in quantities to get a required concentration.

And (*d*) Water to make up to 10 c.c.

The Sorenson values of the test solutions were determined by the quinhydrone method. The results obtained are given in Tables I to VIII.

In measuring the apparent pH values the adjustments with the colorimeter could be made correct to about 0·03 unit in the sensitive range. *The quinhydrone and the indicator methods gave slightly different values for buffered solutions and so an appropriate correction was applied in arriving at the* $-\Delta$pH *values given in the tables.*

TABLE I

Wetting agent: Igepon T. Indicator: Thymol Blue. Ionic strength of buffer = 0.01.

g. of wetting agent in 100 c.c. of the solution	Sorenson value (pH by quinhydrone electrode)	Apparant pH as shown by the indicator	Apparent shift in pH ($-\Delta$ pH)	$K_1 = 2{\cdot}8$; K_2 968 ($-\Delta$ pH theoretical)
1·000	3·24	1·10	2·13	2·41
0·500	3·07	0·97	2·09	2·31
0·200	2·94	0·83	2·10	2·10
0·100	2·88	0·96	1·91	1·88
0·050	2·86	1·10	1·75	1·64
0·020	2·83	1·30	1·52	1·26
0·010	2·83	1·80	1·02	1·02
0·005	2·83	2·17	0·65	0·76
0·000	2·83	2·82	0·00	0·00

TABLE II

Wetting agent: Igepon T. Indicator: Thymol Blue. Ionic strength of buffer = 0·1.

g. of wetting agent in 100 c. c. of the solution	Sorenson value (pH by quinhydrone electrode)	Apparent pH as shown by the indicator	Apparent shift in pH ($-\Delta$ pH)	$K_1 = 19{\cdot}1$; $K_2 = 706$ ($-\Delta$ pH theoretical)
1·000	2·97	1·37	1·53	1·55
0·500	2·90	1·33	1·50	1·52
0·350	2·84	1·33	1·44	1·51
0·200	2·84	1·30	1·47	1·47
0·150	2·84	1·35	1·42	1·44
0·100	2·84	1·40	1·37	1·39
0·050	2·84	1·46	1·31	1·27
0·020	2·84	1·68	1·09	1·04
0·010	2·84	1·94	0·83	0·83
0·005	2·84	2·09	0·69	0·62
0·000	2·83	2·76	0·00	0·00

TABLE III

Wetting agent : Igepon T. Indicator : Bromphenol Blue. Ionic strength of buffer = 0·01

				K_2=6·6
2·00	4·54	3·21	1·41	1·52
1·00	4·41	3·61	0·88	0·88
0·50	4·41	3·82	0·67	0·63
0·35	4·41	3·86	0·63	0·52
0·20	4·39	4·04	0·43	0·37
0·10	4·39	4·22	0·25	0·22
0·05	4·37	4·28	0·17	0·12
0·00	4·36	4·44	0·00	0·00

TABLE IV

Wetting agent : Igepon T. Indicator : Bromphenol Blue. Ionic strength of buffer = 0·1.

g. of wetting agent in 100 c. c. of the solution	Sorenson value (pH by quinhydrone electrode)	Apparent pH as shown by the indicator	Apparent shift in pH ($-\Delta$pH)	K_2=21 (=Δ pH theoretical)
2·00	4·70	3·35	1·51	1·63
1·00	4·70	3·52	1·34	1·34
0·50	4·70	3·80	1·06	1·06
0·20	4·71	4·13	0·74	0·72
0·10	4·71	4·30	0·57	0·49
0·05	4·73	4·43	0·46	0·32
0·00	4·73	4·89	0·00	0·00

TABLE V

Wetting agent : Nekal BX. Indicator : Thymol Blue. Ionic strength of buffer = 0·01.

2·50	3·17	1·52	1·58
1·00	3·00	1·42	1·51
0·50	2·92	1·64	1·21
0·35	2·86	1·90	0·89
0·20	2·86	2·27	0·52
0·16	2·84	2·34	0·43
0·10	2·84	2·40	0·37
0·08	2·84	2·42	0·35
0·04	2·84	2·54	0·23
0·02	2·83	2·61	0·15
0·00	2·83	2·76	0·00

TABLE VI

Wetting agent : Nekal BX. Indicator : Thymol Blue. Ionic strength of buffer = 0·1.

g. of wetting agent in 100 c. c. of the solution	Sorenson value (pH by quinhydrone electrode)	Apparent pH as shown by the indicator	Apparent shift in pH ($-\Delta$ pH)
1·70	2·80	1·22	1·60
0·83	2·63	1·29	1·36
0·45	2·54	1·33	1·23
0·35	2·41	1·42	1·01
0·20	2·41	1·69	0·74
0·18	2·41	1·70	0·73
0·12	2·41	1·96	0·47
0·08	2·41	2·25	0·18
0·04	2·41	2·42	0·01
0·02	2·41	2·42	0·01
0·00	2·40	2·42	0·00

TABLE VII

Wetting agent : Nekal BX. Indicator : Bromphenol Blue. Ionic strength of buffer = 0·01.

2·0	4·42	3·96	0·50
1·0	4·40	4·14	0·30
0·5	4·37	4·34	0·07
0·3	4·37	4·39	0·02
0·1	4·37	4·40	0·01
0·0	4·36	4·40	0·00

TABLE VIII

Wetting agent : Nekal BX. Indicator : Bromphenol Blue. Ionic strength of buffer 0·1.

2·00	4·68	4·20	0·61
1·00	4·70	4·34	0·49
0·50	4·71	4·65	0·19
0·30	4·71	4·77	0·07
0·20	4·71	4·80	0·04
0·10	4·71	4·84	0·00
0·05	4·71	4·85	0·00
0·00	4·71	4·84	0·00

DISCUSSION

1. *The mechanism of displacement of pH.*—After making an extensive qualitative study of the effect of a few paraffin chain salts on a number of indicators, Hartley has suggested that the observed displacement of pH is due to the preferential adsorption of one of the forms of the dye on paraffin chain salt micelles. Indication of pH by a dye is dependent on the equilibrium between the two forms of the dye differing in valence. The equilibrium ratio of the two forms is determined by the pH of the solution. The acid form

of the dye is produced by the union between the basic form and the hydrogen ion. The valence of the acid form is therefore higher algebraically than the valence of the basic form. The various possible types of valence for the two forms are:—

I. Both forms positively charged,
II. Acid form positively charged; basic form uncharged;
III. Acid form uncharged; basic form negatively charged; And
IV. Both forms negatively charged.

The surface active substances can also be divided into the different classes according to the charge possessed by their micelles in solution. When an indicator is added to a solution containing a surface-active agent, there is a possibility that the micelles of the latter may preferentially adsorb one of the forms of the indicator. Normally cationic micelle, however, would not take up any of the indicator of type I and anionic micelle would not adsorb any of the indicator of type IV owing to electrical repulsion; in these cases therefore, the surface-active substance would not affect the determination of pH. This forms the basis of the sign rule of Hartley.[2] In the other cases, there would be a preferential adsorption of one of the forms of the indicator. Owing to the influence of the electric forces, the acid form which has a higher positive charge (or a lower negative charge) would be preferentially taken up by an anionic micelle. The equilibrium between two forms would be consequently displaced, there being a shift towards the acid side. This results in the indication of lower pH. A cationic micelle would behave in the opposite way causing an apparent increase in pH.

In a later paper, Hartley has put forth another mechanism for explaining the displacement of pH brought about by paraffin chain salts when diphenylazo-*o*-nitrophenol is used as indicator. In this case both the forms are almost completely adsorbed by the paraffin chain micelles. The micelle being negatively charged has in its immediate neighbourhood a high concentration of H^+ ions. The indicator therefore finds itself in a region of low pH. The pH indicated therefore is low and gives an idea of H^+ ion concentration near the surface of the micelles. Hartley has shown that there is an approximate correlation between the zeta potential of the micelle got from mobility measurements and that calculated from indicator experiments.

A complete picture of the phenomenon however can only be got by combining both the ideas put forth by Hartley and the following detailed mechanism is therefore proposed in the present paper. The usual indicators are amphipathic substances having both a hydrophobic and hydrophilic portion in the molecule. The surface-active agents are also amphipathic

by nature. When both these types of molecules are present in solution there is a tendency for complex formation. The complex formation is brought about by the union of hydrophobic portion of the indicator with the hydrophobic portion of the molecules or micelles of the surface-active substances. The proportion of the acid and the basic forms of the indicator present in the complex would be controlled by (*a*) the local H^+ ion concentration near the indicator ion and (*b*) the relative life of the two types of the complexes. Due to the difference in the electrical charge associated with the two forms of the indicator, one of the forms may produce a much stabler complex than the other. It is to be pointed out that both the factors act in the same direction in any particular system. A careful study of these factors reveals that a quantitative formulation including these two factors is best done by applying the law of mass action on the basis of activities. Since, however, the activity coefficients are not available for the complicated molecules or micelles dealt with in the present work it is simpler to formulate, employing the concentration terms, and discuss qualitatively the effect of the activity coefficients.

The quantitative aspect of the problem may now be considered. In a solution containing the indicator and the surface-active agent, we have (1) the acid form of the indicator, H In. (2) the basic form of the indicator $In.^-$ (3) the complex between the acid form of the indicator and the surface active ion H In.....W^-. And (4) the complex between the basic form of the indicator and the surface-active substance $In.^-....W^-$. These are in equilibrium. If activity coefficients are not taken into account and if the influence of micelle formation is assumed to be negligible, the following relationship can be formulated. The theory would be applicable to the region wherein micelle formation does not set in or in cases where micelle formation would not effect the general behaviour of the system. Let the total concentration of the indicator be c_i. Let a fraction α be in the free basic form and a fraction β in the free acid form. Applying the law of mass action to complex formation, we get

$$[\text{In}....\text{W}^-] = k_1 c_i \alpha \{cw - [\text{In}^- ....\text{W}^-]\}$$

where k_1 is a constant.

$$\therefore \quad [\text{In}^-....\text{W}^-] = \frac{k_1 c_i \alpha c_w}{1 + k_1 c_i \alpha}.$$

Similarly,

$$[\text{HIn}....\text{W}^-] = \frac{k_2 c_i \beta c_w}{1 + k_2 c_i \beta}$$

where k_2 is a constant. If x and y are the true and apparent pH values respectively, we get,

$$10^{x-pk} = \frac{c_i \alpha}{c_i \beta}$$

and $$10^{y-pk} = \frac{c_i\,\alpha + \dfrac{k_1\,c_i\,\alpha\,c_w}{1+k_1\,c_i\,\alpha}}{c_i\beta + \dfrac{k_2\,c_i\,\beta\,c_w}{1+k_2\,c_i\,\beta}}$$

$$\therefore \quad -\Delta\,\mathrm{pH} = x - y = \log \frac{1+\dfrac{k_2\,c_w}{1+k_2\,c_i\,\beta}}{1+\dfrac{k_1\,c_w}{1+k_1\,c_i\,\alpha}} \tag{1}$$

Now,

$$k_1\,c_i\,\alpha = \frac{[\text{Wetting agent—basic form complex}]}{[\text{Free wetting agent}]}$$

and $$k_2\,c_i\,\beta = \frac{[\text{Wetting agent—acid form complex}]}{[\text{Free wetting agent}]}.$$

These quantities are small as compared with unity since only a small fraction of wetting agent forms the complex. Thus, equation (1) gets reduced to,

$$-\Delta\,\mathrm{pH} = \log_{10} \frac{1+k_2\,c_w}{1+k_1\,c_w} \tag{2}$$

2. *Thymol Blue-Igepon T system.*—(i) The data obtained with the Igepon T-thymol blue system, are found to be in very good agreement with the above theory, as can be seen from Tables I and II. Equation (2) has been used for calculating the theoretical values. The values of k_1 and k_2 have been determined by making use of two of the experimental values of the pH shift.

Apart from the fact that the experimental values can be fitted into the equation, it is to be pointed out that there are other interesting features in the experimental data to show that the theory adequately accounts for the experimental results:—

Igepon T being a sulphonate gives a surface-active ion which is negatively charged. The indicator thymol blue in the acid range has the basic form negatively charged and the acid form uncharged. The acid form consequently gives rise to a stabler complex. Moreover, owing to the Debye effect the negative surface-active ion induces a high local concentration of H^+ ions in the neighbourhood of the complex. Thus the proportion of acid form in the complex would be very high. In equation 3 therefore k_1 would be much smaller than k_2. This is found to be the case.

(0·01 N buffer $k_1 = 2{\cdot}8$; $k_2 = 968$,

0·1 N buffer $k_1 = 19$; $k_2 > = 706$)

(ii) At sufficiently high concentrations of the wetting agent, complex formation may be more or less complete; and consequently the pH shift would be practically independent of concentration. This has been found to be the case.

(iii) At low values for $k_1 c_w$, equation 3 becomes,

$$- \Delta \text{ pH} = \log_{10} (1 + k_2 c_w) \qquad (3)$$

It can be deduced from equation 3 that if a pH shift of 0·3 is produced by a certain concentration c_1 of the wetting agent (*a*) a shift of 1·0 unit would be produced by a concentration 9 c_1 and (*b*) a shift of 2·0 units would be brought about by a concentration 99 c_1. These conclusions hold within the limits of the experimental error in the experiments with 0·01 N buffer solutions. With 0·1 N buffer solutions also the relation (*a*) is satisfied. The relation (*b*) is not obeyed since $k_1 c_w$ becomes comparable with unity when c_w is equal to 99 c_1.

3. *The bromphenol blue-Igepon T system.*—It is known that the acid form of bromphenol blue has a single negative charge while the basic form has a double negative charge. According to Hartley, there should be no shift in pH with this indicator, when a surface-active substance of the type of Igepon T (which has a surface-active anion) is added.[2] Hartley based his conclusions on the idea that complexes between like charged molecules was improbable. But, the experiments recorded in this paper show that there is a considerable displacement of pH in the present case. This shows that in spite of the electrical repulsion between like charged molecules, complex formation between them does occur owing to the strong attractive forces between the hydrophobic portion of the wetting agent ion and that of the indicator ion. It may, however, be expected that complex formation would be relatively low; this would be especially true of the basic form which bears two negative charges. One may therefore apply equation 3 which corresponds to the existence of the complex only with the acid form. The calculated values of $- \Delta$pH on the basis of this equation and the corresponding experimental values are given in Tables III and IV. An examination of the tables shows that the experimental data support the theory. The other interesting features which support the thoery are:—

(*a*) The values of k_2 for bromphenol blue are much lower than the corresponding values for thymol blue showing that complex formation is much less in the former case. This is but to be expected since the acid form of the former indicator which forms the complex is negatively charged, whereas that of the latter indicator is uncharged.

(*b*) For the reason indicated above, the complex formation with bromphenol blue may be expected to be incomplete even at very high concentration of the wetting agent. This is in agreement with the experimental data.

(*c*) The conclusions drawn from equation 3 for thymol blue, also hold for bromphenol blue. The concentration of wetting agent required to effect a shift of unity in pH is about 9 times the concentration required to cause a shift of 0·3 unit.

(*d*) The shift in pH is found to be practically independent of indicator concentration

4. *Effect of ionic strength on the pH shift.*—A comparison of tables I and II shows that an increase in ionic strength diminishes the pH shift in the case of thymol blue. At lower concentrations of wetting agent, the effect of salts is small whereas it becomes considerable at high concentrations. The effect can be quantitatively treated on lines similar to the treatment of neutral salt effect in reaction kinetics.[6] The exact magnitude of the effect however cannot be calculated since the value of β in the equation, of Bronsted[6] is not known for the differennt molecules. Due to the "a terms", however (which correspond to the zeta potential effect of Hartley) k_1 would increase whereas k_2 would be unaffected. Experimentally this is found to be approximately the case. This explains, in fact, why at low concentrations of the wetting agent (where k_1 does not enter the equation), the effect of ionic strength is small. It is of interest to note that k_2 does decrease to some extent with increase of ionic strength. This decrease of the value of k_2 shows that the life of the complex from the acid form of the indicator is appreciably decreased by increase in the ionic strength. This is somewhat surprising since the acid form of thymol blue is known to be uncharged (from the simple theory of the neutral salt effect) and should not be affected by ionic strength. It is to be noted however that the acid form of the indicator has a "Zwitterion" constitution and the observed effect only shows that the wetting agent ion is nearer to the positive charge of the "Zwitterion" than to the negative charge; this is but to be expected in view of the flexible nature of the hydrocarbon chain in Igepon T, which would help the orientation of its charged end to a position of minimum potential energy.

At high concentrations of Igepon T where the complex formation is more or less complete, a change of ionic strength from 0·034 (in 1 per cent. solution of Igepon T in 0·01 N buffer) to 0·12 (in 1 per cent. solution of Igepon T in 0·1 N buffer), decreases the pH shift by about 0·6 unit. It is of interest to note that this corresponds very nearly to the effect of ionic

strength (c.a. 0·55 unit) observed by Hartley in the system investigated by him (indicator: diphenylazo-*o*-nitrophenol; surface-active substance: triethanol-ammonium cetane sulphonate). This shows that the changes in potential in the neighbourhood of the complex brought about by salts are almost the same in the two systems.

A few experiments were tried with a view to get the maximum possible pH shift. It was possible to get as high a shift as 2·4 units by having the wetting agents at a concentration of 0·2 per cent. in water and adjusting the pH to 4·2 (quinhydrone electrode) by adding acetic acid.

With bromphenol blue, increase in ionic strength *increases* the pH shift. This surprising feature is just the opposite of what has been observed in the present work with thymol blue and by Hartley and Roe with diphenylazo-o-nitrophenol. This effect can be explained as follows:—As is already pointed out, the basic forms of the indicator which bears two negative charges, does not form any complex at all due to strong electrical repulsion. Increase of ionic strength no doubt decreases electrical repulsion; but the repulsion is yet too strong (at ionic strength $= 0 \cdot 1$) for any complex formation. Thus the basic form does not play any role in bringing about the observed effect. For the same reason the observed pH changes are entirely determined by k_2 and follow equation (4). Complex formation of the acid form of the indicator however, is enhanced by the increase in ionic strength due to diminution in the electrical repulsion and thus causes the observed effect.

5. *Nekal BX-Thymol Blue System.*—An examination of the data in Tables 5 and 6 shows that the theory worked out for Igepon T is not applicable to the present system. In the present case there is a certain concentration of the wetting agent at which the pH shift begins to increase considerably with concentration. This concentration value is 0·2 to 0·3 per cent. with 0·01 N buffer and 0·04 to 0·08 per cent. with 0·1 N buffer. There is a striking coincidence between these values and the micelle formation concentrations got from surface tension studies[4] (*viz.*, 0·07 per cent. in 0·1 N buffer and 0·27 per cent. in 0·01 N buffer). In this system the micelles appear to be much more effective than the single molecules in bringing about the pH shift. The complex formation is not as strong as with Igepon T since Nekal BX is relatively a short molecule and the electrical repulsion between the two negatively charged portions in the complex is consequently strong.

6. *Nekal BX-Bromphenol Blue System.*—The displacement of pH in the above system is very small. This is to be expected for (*a*) Nekal BX is

a short molecule and hence electrical repulsive forces would be strong rendering the complex relatively unstable and (*b*) bromphenol blue having both the forms negatively charged would not be taken up by the wetting agent to any large extent. Since the shift is very small, no discussion of the quantitative aspect is possible. It may, however, be pointed out that the shift is marked, only at concentrations higher than at which micelle formation has occurred.

7. *Wetting power and pH shift.*—Since wetting action and the pH shift both involve the union of hydrophobic portions, it may be expected that there should be a general correlation between pH shift and wetting power. An extensive investigation is desirable from this point of view. The observations in the present work show that Igepon T is a much better wetting agent than Nekal BX, a conclusion which is also supported by surface tension studies[4].

SUMMARY

1. There is an apparent shift towards the acid side in the pH of buffered solutions as measured by the use of the indicators, thymol blue and bromphenol blue when wetting agents like Igepon T and Nekal BX are present in the system.

2. Igepon T shows a very large shift with thymol blue. Under favourable conditions the shift may be as large as 2·4 units, an effect much bigger than what has been reported in literature so far for any system; Nekal BX shows less of the pH shift. Both the wetting agents affect bromphenol blue to a smaller extent.

3. A quantitative investigation of the phenomenon has been made. A theory has been put forth, based on the formation of a complex between the wetting agent and the indicator to account quantitatively for the effect of concentration of the wetting agent on the pH shift.

4. Igepon T shows a marked shift with bromphenol blue as well. This forms a clear exception to the sign rule of Hartley.

5. Increase in ionic strength decreases the pH shift with thymol blue as it is the case with the system worked by Hartley and Roe. When bromphenol blue is used neutral salts produce an opposite effect. An explanation is offered which account for these diverse results.

6. The variation of pH shift with concentration of Nekal BX with thymol blue indicates that micelle formation of the wetting agent occurs rather suddenly.

7. The possible relationship between the pH shift and wetting power is pointed out.

References

1. Smith and Jones .. *J. Phys. Chem.*, 1934, 243.
2. Hartley .. *Trans. Far. Soc.*, 1934, **30**, 444.
3. Hartley and Roe .. *Ibid.*, 1940, **36**, 106.
4. Krishnappa, Doss and Rao *Proc. Indian Acad. Sci.*, **1946, 23**, 1.
5. Britton .. *Hydrogen Ions.*
6. *Cf.* Taylor .. *A Treatise on Physical Chemistry*, **2**, Second Edition, p. 1002.

CONSTITUTION OF KANUGIN—PART II

By S. Rajagopalan, S. Rangaswami, K. Visweswara Rao and T. R. Seshadri

(From the Department of Chemistry, Andhra University)

Received December 29, 1945

In Part I[1] were described certain earlier experiments which could not be continued due to the war and the dislocation of our laboratories. It was, however, shown that kanugin is a flavone derivative giving the characteristic colour reactions and that it has a resorcinol unit since it yielded *p*-methoxy-salicylic acid on oxidation with permanganate or decomposition with alkali. The reaction with hydriodic acid could not be explained as simple demethylation since nor-kanugin did not regenerate kanugin on re-methylation but yielded a different substance. Further work has now been possible and particulars regarding the complete constitution of kanugin are described in this paper.

Subsequent to our last publication it has been found that in the root bark of *Pongamia glabra* kanugin is accompanied by another related substance and careful and repeated crystallisation is necessary in order to remove it and obtain kanugin quite pure. The second component seems to be more in abundance in thicker and more mature roots that have been used in later work. Consequent on this thorough purification, the melting point of kanugin has been raised to 203–05° and its analysis is found to agree more closely with the formula $C_{19}H_{16}O_7$. Further with concentrated sulphuric acid and a crystal of gallic acid it gives a bright green colour characteristic of a methylene-dioxy grouping.

Degradation with alkali has been investigated in detail. A repetition of the fission of kanugin with aqueous potash has yielded two acid products which could be separated by means of their marked difference in solubility in water. The less soluble one is identified as myristicic acid by analysis, colour reaction, and by comparison with an authentic sample prepared starting from oil of nutmeg. The more soluble portion is found to be the same as the impure form of *p*-methoxy-salicylic acid mentioned in Part I. This identification has been confirmed by the convertion of the product into the 5-bromo-derivative and subsequent esterification to form the methyl ester of 5-bromo-4-methoxy-salicylic acid. These derivatives could be easily obtained pure since they are sparingly soluble, and they are found to be identical with authentic samples prepared from synthetic 4-methoxy-salicylic acid.

Degradation using absolute alcoholic potash has gone much better and yielded myristicic acid and ω: 4-dimethoxy-2-hydroxy-acetophenone in good yields. From these results it is clear that kanugin is a robinetin derivative and that it has a methylenedioxy group in the 3′: 4′-positions, the other three hydroxyl groups being protected by methyl groups (I).

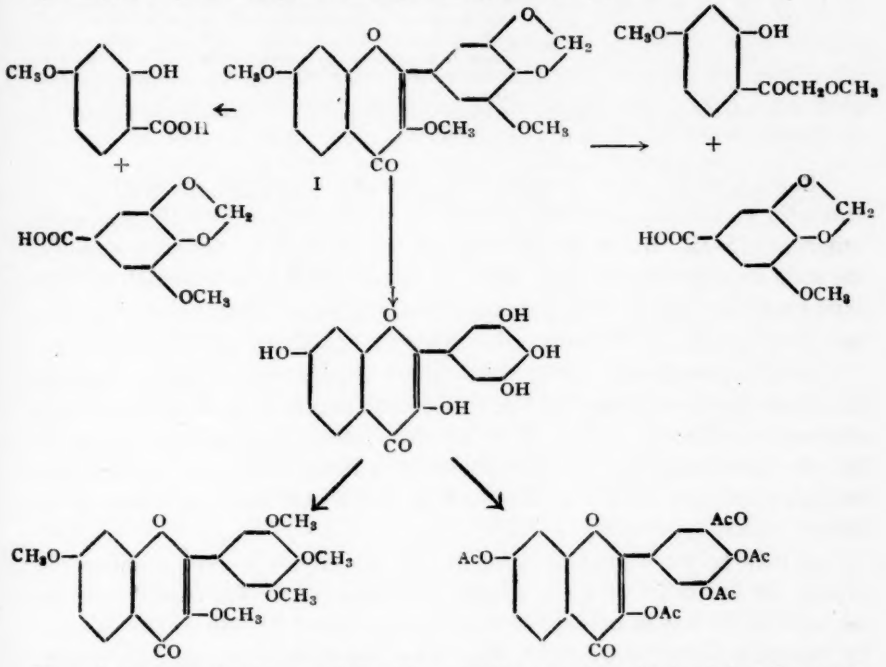

The above constitution explains the peculiar results obtained by the treatment of kanugin with hydriodic acid and the re-methylation of nor-kanugin.

When purified kanugin is employed, the nor-kanugin obtained has slightly different properties from those already recorded. It is a yellow crystalline substance melting at about 325° with decomposition and its composition corresponds with the formula $C_{15}H_{10}O_7$. Its pentamethyl ether melts at 148–49° and its penta-acetate at 223–25°. Its identity with robinetin has been established by comparison with a synthetic sample obtained by the method of Allan and Robinson, starting from ω-methoxy resacetophenone and the sodium salt and anhydride of *O*-trimethyl gallic acid, followed by demethylation.[2] Mixed melting point determinations of the flavonols and their derivatives have been made as also a comparison of the colour reactions of the two samples under identical conditions. The data are presented in the following table.

Property	Nor-kanugin	Robinetin
1. Melting point of the flavonol ..	320–25°	320–25°
2. Colour with $FeCl_3$ ..	Dark olive brown	Dark olive brown
3. Precipitate with lead acetate ..	Red	Red
4. Colour changes at pH 11 ..	Quickly dissolves to a yellow solution, changes to emerald green in 10 seconds, then to greenish blue and pure blue, changes further to violet and finally pink, resembling alkaline phenolphthalein. This colour is stable for an hour and fades to brown through brown pink	
5. Melting point of the methyl ether	135–36° and 148–49°	135–36° and 148–49°
6. Melting point of the acetate ..	223–25°	223–25°

Some samples of the pentamethyl ether of nor-kanugin (natural) and of robinetin (synthetic) have been found to be melting at 148–49° and some others at 135–36°. But in the latter case, when the melt is allowed to solidify, the solid subsequently melts at 148°. A mixture of the low and high melting samples melts only at 148°. It may therefore be concluded that there are two forms of the solid methyl ether having two different melting points.

In the constitution of kanugin given above, two important features should be noted. Kanugin belongs to the small number of naturally occurring anthoxanthin derivatives in which all the hydroxyl groups are protected. But the more important point is the use of a methylene group for this protection, this being the first instance where this group has been found in the flavone series.

It may be interesting to compare the crystalline flavonol components present in the different parts of the Pongamia tree. The seeds[3] contain karanjin which may be considered to be a derivative of 3 : 7-dihydroxy-flavone, *i.e.*, derived from resorcinol. The constitution of the other crystalline substance pongamol, also present in the seeds, is not yet clearly known. Kæmpferol is found in the flowers.[4] It is also a flavonol but is derived from phloroglucinol. The constitution of pongamin which is found in very small amounts in the flowers is still unknown. The root bark[5] contains kanugin which is again a flavonol derived from resorcinol but the side-phenyl nucleus is in a higher state of oxidation. Another noteworthy feature is that in the flowers the protection of the hydroxyl groups is the least whereas in the roots it is complete; an efficient mechanism should therefore be available in this part of the plant for this protection.

Experimental

Kanugin.

The sample of kanugin obtained from the root bark of ***Pongamia glabra*** was crystallised using excess of alcohol in which it is sparingly soluble. The

light colourless crystalline solid that was produced after two crystallisations melted between 196 and 200°. For further purification it was again crystallised twice using a mixture of alcohol and acetic acid. It then came out as colourless brittle rectangular plates and needles with a pearly lustre melting at 203–05°. Further crystallisation did not raise the melting point [Found: C, 63·8; H, 4·7; OCH_3, 25·8; $C_{19}H_{16}O_7$ requires C, 64·0; H, 4·5; OCH_3 (3), 26·1%]. It dissolved in concentrated sulphuric acid to give a bright yellow solution and the colour changes and fluorescence were exhibited as reported previously. Even an alcoholic solution gave a blue-violet fluorescence; with magnesium and hydrochloric acid a brilliant scarlet red colour was produced. When gently warmed with a solution of gallic acid in concentrated sulphuric acid, a deep emerald green colour was obtained in 10 seconds.

Alkaline Hydrolysis of Kanugin.

(1) ***Using aqueous alcoholic potash.***—Kanugin (0·5 g.) was dissolved in aqueous alcoholic potash (alcohol 40 c.c., water 40 c.c. and potash 5 g.) and the solution boiled under reflux for 6 hours in an atmosphere of hydrogen. It was then cooled, acidified with hydrochloric acid and the alcohol distilled off under reduced pressure. The residue was then extracted repeatedly with ether. The ether solution was then shaken first with aqueous sodium bicarbonate in order to separate acid products (A) and subsequently with dilute sodium hydroxide to remove phenolic components (B). Neutral products would then be left in the ether solution (C). (B) and (C) were found to be insignificant in amount and were not further studied.

On acidifying the bicarbonate extract a solid separated out. This was washed with water and marked (D). By ether-extracting the solution the more soluble part was isolated (E). When (D) was crystallised from dilute alcohol it melted at 212–13° and had the appearance of long rectangular plates and prisms with a tendency to taper at the ends (Found: C, 55·3; H, 4·4; OCH_3, 16·3; $C_9H_8O_5$ requires C, 55·1; H, 4·1 and OCH_3, 15·8%). It formed a yellow solution in concentrated sulphuric acid; when a crystal of gallic acid was added and the solution gently warmed the colour changed to bright emerald green and finally to a stable pure blue. The mixed melting point with an authentic sample of myristicic acid prepared from oil of nutmeg was not depressed.

When (E) was crystallised from boiling water it yielded a colourless crystalline product (flat needles) which had an indefinite melting point (130–45°), gave a purple colour with ferric chloride and had all the properties of a similar sample (4-methoxy-salicylic acid) already reported in Part I.

The substance (0·2 g.) was dissolved in glacial acetic acid (3 c.c.) and treated with a slight excess of a solution of bromine in acetic acid. The solution was rapidly decolourised and on keeping the mixture for a few hours at 0° a crystalline solid separated out. It was filtered and washed with a little water. Since it was very sparingly soluble in solvents it was purified by boiling with glacial acetic acid. It then melted at 258–59° with sintering a little earlier and had the appearance of small rectangular plates (Found: C, 38·8; H, 3·1; $C_8H_7O_4$ Br requires C, 38·9; H, 2·8%). It was identical with a sample of 5-bromo-4-methoxy-salicylic acid prepared from a pure sample of 4-methoxy-salicylic acid.

The bromo acid was esterified by boiling with anhydrous methyl alcohol and a little concentrated sulphuric acid for 12 hours. On allowing to stand overnight crystals of the ester separated out. When recrystallised from methyl alcohol-acetic acid mixture it came out in the form of rhombohedral plates melting at 145–46°, agreeing with the description of the ester by Potter Rice[6] who obtained it by a different method.

(2) *Using absolute alcoholic potash.*—Kanugin (0·75 g.) was treated with absolute alcoholic potash (30 c.c. of 8% solution) and the mixture refluxed for 6 hours under anhydrous conditions. The solid did not go into solution easily and only after 2½ hours solution was complete. After 6 hours, the solvent was completely removed, water (30 c.c.) added and the solution filtered through a plug of cotton-wool. When the filtrate was acidified, a crystalline solid separated in good yield. The solution along with the solid was extracted with ether twice and the ether solution shaken with aqueous sodium bicarbonate to separate the acidic component (A). The ether layer was finally washed with water and evaporated. The residue was a liquid which soon solidified. It was filtered, washed with a little water and crystallised twice from hot water when it came out as colourless thin rectangular plates melting at 65–67°. Mixed melting point with an authentic sample of ω: 4-dimethoxy-2-hydroxy-acetophenone was undepressed. It gave a reddish brown colour with ferric chloride and did not respond to the methylenedioxy group test. The 2: 4-dinitrophenyl-hydrazone of the ketone prepared in the usual manner was crystallised from ethyl acetate, when it came out as bright red rectangular plates. It melted at 218–20° alone or when admixed with the 2: 4-dinitro-phenylhydrazone of synthetic ω: 4-dimethoxy-2-hydroxy acetophenone.

On acidifying the bicarbonate extract (A) with hydrochloric acid a crystalline solid was obtained. It was filtered, washed with a little water and purified by crystallising twice from methyl alcohol from which it sepa-

rated as big rectangular prisms with a tendency to taper at the ends and melting at 212–14°. This was identical with myristicic acid obtained in the other method of hydrolysis

Demethylation of Kanugin: *Nor-Kanugin* (*Robinetin*).

A solution of kanugin (0·5 g.) in phenol (3 c.c.) was treated with hydriodic acid (10 c.c. of d. 1·7). The mixture was heated at 150–60° for 1 hour. It was then cooled, diluted with water (50 c.c.) and free iodine decomposed by means of sodium sulphite. The yellow solid that separated out was filtered, washed repeatedly with hot water and purified by crystallising it from aqueous alcohol when it came out as yellow rectangular plates, melting at 320–25° with decomposition (Found in the air-dried sample: C, 55·9; H, 4·1; $C_{15}H_{10}O_7$, H_2O requires C, 56·2; H, 3·7%). The compound was sparingly soluble in hot water and moderately in alcohol and acetic acid. Its alcoholic solution exhibited a brilliant green fluorescence. It gave a dark olive green colour with ferric chloride and a red precipitate with lead acetate in alcoholic solution. In concentrated sulphuric acid it dissolved to form a yellow solution without fluorescence.

Nor-Kanugin Acetate

The acetate of nor-kanugin was prepared by boiling it (0·1 g.) with acetic anhydride (3 c.c.) and a drop of pyridine for an hour and a half. The anhydride was then removed under reduced pressure and the white solid left behind was purified by crystallisation from absolute alcohol. It came out in the form of colourless narrow rectangular prisms, melting at 223–25°. The mixed melting point with a sample of the acetate of robinetin was not depressed (223–25°).

Nor-Kanugin Methyl Ether

A solution of nor-kanugin (0·1 g.) in anhydrous acetone (25 c.c.) was treated with dimethyl sulphate (0·3 c.c.) and anhydrous potassium carbonate (2 g.). After refluxing for 8 hours, the potassium salts were filtered off and the residue washed with a little acetone. When the solvent was distilled off, the methyl ether was obtained as a white crystalline solid. It was purified by crystallisation from alcohol when it appeared as narrow rectangular plates melting at 148–49°; the mixed melting point with *robinetin* methyl ether (synthetic) was undepressed (Found in the air-dried sample: C, 61·9; H, 6·0; OCH_3, 38·9 and loss on drying *in vacuo* 5·0. $C_{20}H_{20}O_7$, H_2O requires C, 61·5; H, 5·6; OCH_3 39·7 and H_2O loss 4·6. Found in samples dried at 110° *in vacuo*: C, 64·9, H, 5·5; $C_{20}H_{20}O_7$ requires C, 64·5; H, 5·4%).

Summary

Kanugin $C_{19}H_{16}O_7$ yields myristicic acid and *p*-methoxy salicylic acid when decomposed with aqueous alcoholic potash and myristicic acid ω: 4-dimethoxy-2-hydroxy-acetophenone when decomposed with absolute alcoholic potash. Nor-kanugin has been identified as robinetin by a comparison of the flavonols and their derivatives. It is, therefore, concluded that kanugin is 3:7:5′-trimethoxy-3′:4′-methylenedioxy-flavone. The crystalline components of the seeds, flowers and root bark of *Pongamia glabra* are compared.

References

1. Rangaswami and Seshadri .. *Proc. Ind. Acad. Sci.* (A), 1943, **17**, 20.
2. Badhwar, Kang and Venkataraman .. *J. C. S.*, 1932, 1105.
   Charlesworth and Robinson .. *Ibid.*, 1933, 268.
   Gulati and Venkataraman .. *J. Prakt. Chemie*, 1933, **137**, 53.
3. Rao, Rao and Seshadri .. *Proc. Ind. Acad. Sci.* (A), 1939, **10**, 65.
   Rangaswami and Seshadri .. *Ibid.*, 1942, **15**, 417.
4. Murti and Seshadri .. *Ibid.*, 1944, **20**, 279.
5. Rangaswami, Rao and Seshadri .. *Ibid.*, 1942, **16**, 319.
6. Potter Rice .. *J. A. C. S.*, 1926, 3125.

A NOTE ON SPECTRAL INTENSITY CHANGES IN HIGH-FREQUENCY GLOW DISCHARGE IN AIR

By N. R. Tawde, F.A.Sc., and G. K. Mehta

(Physics Laboratories, Royal Institute of Science, Bombay)

Received September 20, 1945

Asundi and J. Singh[1] have recently drawn some important conclusions about the relative strengths of the first positive and second positive band systems of nitrogen excited by h.f. discharge in rarefied air. They observed a change in the colour of the glow when the frequency of oscillation was changed. This happened abruptly at a critical frequency of 735 k.c. below which the first positive system is stronger than the second positive system and above which the reverse is true. The change in colour is attributed by them to the change in intensities of these two band systems.

The authors have referred to the work of Brasefield[2] who has investigated the variations in the electron velocity in the h.f. discharge. He extrapolated the velocity of the exciting electrons in the h.f. discharge from the curves (got from independent experiments) representing the variation in the ratio of the intensities of two neighbouring lines with the uniform velocities of the electrons employed for excitation. This method will be correct if the discharge gives rise to uniform electron velocities. This is not true as the electrons undergo a velocity distribution in the h.f. discharge. Thus it is not possible to draw any quantitative conclusion regarding the mean electron velocity from the above method. The deviations of Brasefield's results from the actual values of the electron velocities, occurring in the h.f. discharge, cannot be estimated unless some new method is tried which takes into consideration the distribution of electron velocities. The general conclusions about (1) the increase in electron velocity with the decrease in the frequency of oscillation; (2) the increase in electron velocity with the increase in excitation voltage; (3) the decrease in electron velocity with the increase in pressure, may be true but no qualtitative conclusions are possible.

Asundi and J. Singh have assumed that the output voltage of the oscillator was constant for all the frequencies. This is contrary to our experience of Hartley circuits. The output voltage varies considerably with the change in frequency. At the same time the conductivity of the discharge being different at different frequencies, the load on the oscillator will vary at

different frequencies and may cause a change in the output voltage. It is known that unless the Hartley circuit is meant to deliver a considerably high power the output voltage changes with the load. Data with regard to the modified Hartley circuit used by Asundi and J. Singh giving a constant voltage output at different frequencies and loads would have facilitated the correctness of the above assumption. It would have been better if the constancy of voltage was checked and its absolute value noted. These conditions being not defined, it is quite likely that the change in the electron velocity which is responsible for the change in the relative intensities of the two band systems may be due partly to the change in voltage and partly to the change in frequency or to the change in voltage only.

Again there is no mention of the pressure at which the investigations were made and this is a very significant factor. According to Brasefield's simplified mechanism of the h.f. discharge, a decrease in frequency will increase the electron velocity, because the time for which electric force will act on the electron will be longer at lower frequency. If this is correct, then with a known change in frequency the resulting change in the electron velocity will depend on the mean free path of the electron and thus on the pressure. This change in electron velocity with a known change in frequency will also depend on the voltage of excitation as the velocity will depend on the electric force acting on it. Thus for a particular applied voltage, there will be a pressure above which a change in frequency will not change the electron velocity. This will be when the m.f.p. for the electron will be smaller than the distance travelled by it in the time of half a cycle at the highest frequency. Asundi and Pant[3] have also observed that the phenomena get complicated at high pressures. This is due to the small m.f.p. of the electrons at high pressures.

A phenomenon of the colour change in the glow of the h.f. discharge in air was lately observed by us while doing probe study of the h.f. discharge. The frequency range was higher than that used by Asundi and J. Singh (4 to 15 m.c.). A sudden change in colour was observed when the pressure in the discharge tube was being lowered. The change was abrupt at a certain pressure. The value of this critical pressure was found to vary with excitation voltage as well as the frequency. In view of this, it appears that the change in colour is a complicated phenomenon associated with several parameters like pressure, frequency, excitation voltage, etc. As an example, the following Tables I and II will give an idea as to how either of these parameters is susceptible to change with variation in the other. The observations given here were taken with a cylindrical tube having external sleeve electrodes.

TABLE I

Frequency in megacycles sec.	Critical Pressure in mm. at	
	1000 V	1300 V
12	0·24	0·54
9	0·34	0·69
7	0·40	0·76
4	0·51	0·89

TABLE II

Voltage	Critical Pressure in mm. at Frequency	
	4 mc./sec.	9 mc./sec.
800	0·20	..
1000	0·51	0·34
1250	0·73	0·56
1400	0·85	0·68

The tube was connected through drying system and oil manometer to a Cenco Hyvac pump. The discharge was excited by h.f. oscillations from a Hartley circuit, the frequency of which was changeable from 4 to 15 megacycles. The h.f. voltages were measured by a thermionic voltmeter specially designed for the purpose. The frequency was measured by a General Radio absorption type of wavemeter. Table I gives the variation of critical pressure with frequency of oscillation at two excitation voltages; while Table II shows its variation with the voltage at two different frequencies.

We agree that the relative changes in the two band systems as observed by Asundi and J. Singh may have been brought about by a change in electron velocity, but whether the critical velocity can be attributed to a change in frequency alone is a doubtful point in the absence of data about the other variables. For some time we have been investigating several other aspects of h.f. discharge quantitatively, the results of which will be communicated in due course.

REFERENCES

1. Asundi and J. Singh .. *Proc. Ind. Acad. Sci.*, 1945, **22**, 60.
2. C. J. Brasefield .. *Phys. Rev.*, 1929, **33**, 925 ; 1930, **35**, 92 and 1073.
3. Asundi and Pant .. *M.Sc. Thesis, Benares Hindu University.*

RADIATION BALANCE OF THE LOWER STRATOSPHERE

Part I. Height Distribution of Solar Energy Absorption in the Atmosphere

By R. V. Karandikar, M.Sc.

Received November 10, 1945

(Communicated by Dr. K. R. Ramanathan, F.A.SC.)

Abstract.—A study of the radiation balance of the atmosphere involves the determination of the absorption and emission of radiant energy due to the different constituents of the atmosphere. In the stratosphere below 50 km., these are mainly ozone, CO_2 and water vapour. The major part of the absorbed energy is from solar radiation, the actual absorption at different levels being determined by the absorption coefficients of these gases and their vertical distributions. In this paper, a detailed survey is made of all the available data and of the recent methods developed for using such data, and after proper selection, curves are prepared giving the solar energy absorbed by different quantities of O_3, CO_2 and H_2O. These are used to calculate the absorption of solar energy per unit volume and per unit mass in different 2 km. layers for certain vertical distributions of the constituents. It is seen that the mass density of absorption due to ozone above 50 km. becomes much larger than that due to CO_2 and H_2O while in the region below 30 km., they become comparable. Water vapour becomes more and more effective as we approach the earth.

§ 1. Introduction

The investigation of the important problem of radiation balance of the earth's stratosphere involves the study of the absorption and radiation of energy due to the different absorbing constituents of the atmosphere. Gowan[1] has worked out in two papers the effect of ozone on the temperature of the upper atmosphere. At the time when he wrote his papers, little was known about the detailed height distribution of atmospheric ozone. Later work by Götz, Meetham and Dobson,[2] Regener,[3] and the American workers[4] has provided important knowledge about this. Penndorf[5] has used some of these results to calculate the heating and cooling of the ozonosphere. But he considered only the ultra-violet absorption due to ozone, without taking into account the visible absorption in the Chappuis band which also plays a part, and neglected the effect of carbon dioxide and water vapour. In a

later paper, Godfrey and Price[6] have investigated ' the thermal radiation and absorption in the upper atmosphere ' but have concerned themselves mainly with the ionosphere above 100 km., where the main absorbing constituent is oxygen. On the other hand, Elsasser[7e] in his recent investigation of ' the heat transfer by infra-red radiation in the atmosphere ' mainly deals with the region below about 10 km., where water vapour is the predominant absorbing substance. As far as the lower stratosphere is concerned, it is clear that the absorption and emission of radiation is governed almost entirely by ozone, carbon dioxide and water vapour.[8] Oxides of nitrogen and some polyatomic gases like methane, ethylene, etc., which have some absorption bands, usually occur in variable and very small quantities and are probably unimportant. Recent investigations of atmospheric absorption in the infra-red by Adel and Lampland,[9] the study of the water vapour spectrum by Weber and Randall[10] and of CO_2 absorption in the infra-red by Martin and Barker,[11] and the development of methods of using such data introduced by Schnaidt,[12] Elsasser,[7] Callendar,[13] and Strong[14,15] supply important material for a reconsideration of the subject.

The total inflow of radiant energy from different sources into any layer of the atmosphere consists of (i) the incident solar radiation, (ii) the terrestrial radiation from the surface of the earth, and (iii) the radiation from the different atmospheric layers above and below the layer under consideration, which depends upon their composition and temperature. The loss of radiation by the layer consists of the radiation from both sides of the layer, assuming it to radiate at its temperature in those regions where it has selective absorption and in proportion to its effective absorption coefficient. The difference between the absorption and emission by the layer will give the net radiation used up in heating the layer, and if there is radiation balance, this quantity will be zero. This is equivalent to the condition that at any level in the atmosphere where there is radiation balance, the incident solar energy flux is equal to the net upward flux due to radiation from all the gaseous layers and the earth.

The investigation therefore can be divided into the following sections:—

(i) An examination of the nature and amounts of the different absorbing gases at different levels in the atmosphere. We shall confine our attention to the region below 50 km.

(ii) Collection and selection of the necessary data regarding the absorption coefficients of the constituent gases throughout the spectrum.

(iii) Calculation of the vertical distribution of solar energy absorption in the atmosphere.

(iv) Preparation of radiation charts for the three main gases (ozone, carbon dioxide and water vapour) of the atmosphere below 50 km., suitable for calculating the net radiation from a given column of absorbents.

(v) Calculation of the equilibrium temperatures for known vertical distributions of ozone like those at Tromsø, Arosa, Poona, etc., and assumed distributions of CO_2 and water vapour.

It is the purpose of this paper to consider the absorption side of the problem, covering the first three items. The radiation side and the linking up of the two sides will be taken up later in two papers.

§ 2. The Solar Energy Curve

The solar energy received at the earth is a parallel beam radiation. The intensity of the incident solar radiation outside the earth's atmosphere is calculated by using Planck's relation on the assumption that the sun radiates as a black body at 6000° K. This gives the total energy radiated out from unit area of the sun's disc as:

$$R = \sigma T^4 = 1767 \cdot 6 \text{ cal. cm.}^{-2} \text{ sec.}^{-1}$$

The energy received at the outer limit of the earth's atmosphere will be the solar constant, S, and is given by

$$S = R \cdot r^2/D^2 = 2 \cdot 306 \text{ cal. cm.}^{-2} \text{ min.}^{-1},$$

where r is the sun's radius and D the earth's mean distance from the sun. This is considerably higher than the observed value, *viz.*, 1·925 cal. cm.$^{-2}$ min.$^{-1}$, the mean value given by Abbot.[16] Abbot's value is however obtained neglecting the absorption of solar energy by ozone in the ultra-violet (Hartley) band which is about 6·26%. Including this, S becomes 2·045 cal. cm.$^{-2}$ min.$^{-1}$ Still there is discrepancy between this value and the above calculated value. This is due either to the sun's assumed effective temperature (6000° K.) being too high, or the fact that the sun might not be radiating strictly as a black body.[17] In all further calculations, the sun is taken as a black body at 6000° K. and the solar constant as 2·045 cal. cm.$^{-2}$ min.$^{-1}$, which is Abbot's value corrected as mentioned above; thus the solar energy received by one sq. cm. at the outer limit of the earth's atmosphere is given by simply multiplying the corresponding energy radiated from one sq. cm. of the sun's disc by the factor: $S/R = 1 \cdot 929 \times 10^{-5}$. This is equivalent to taking the effective temperature to be nearly 5823 ° K. for the total radiation and, rather inconsistently, to be 6000° K. for the distribution of radiant energy in the solar spectrum. Any error that might be caused in doing so will be of a numerical nature, and can easily be corrected by making a corresponding slight change in the above multiplying

factor. Tables I, II, III give the solar energy contained in the different absorption bands of ozone, CO_2 and water vapour, as it is received at the outer limit of the earth's atmosphere.

§ 3. Ozone Bands

(1) *Ultra-violet (Hartley) Band:* 2000-3300 Å.—(*a*) Data by Meyer,[18] Läuchli,[19] Fabry-Buisson,[20] Ny Tsi-Ze and Choong[21] are available. Those by the last named authors (Fig. 1) were used as being the most detailed.

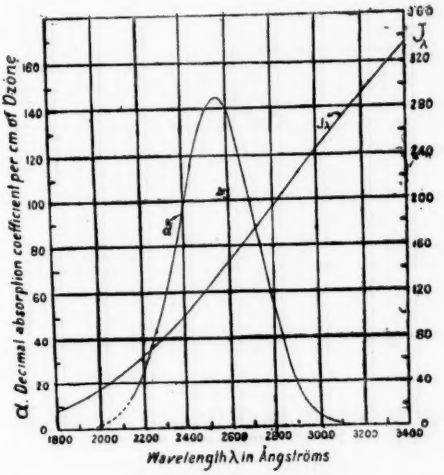

Fig. 1. α, the decimal absorption coefficient per cm. of ozone at N.T.P. in the Hartley band according to data by Ny Tsi-Ze and Choong Shin-Piaw. J_λ is the intensity of the incident solar radiation just outside the earth's atmosphere.
Unit of $J_\lambda d\lambda$ = cal. cm.$^{-2}$ sec.$^{-1}$

The curve gives the decimal absorption coefficient α per cm. of ozone at N.T.P. at different wavelengths, Beer's law ($I = I_0 \times 10^{-\alpha s}$) being assumed to hold for each wavelength. Curves were prepared, using Beer's law, giving absorption from wavelength to wavelength due to known quantities of ozone. The transmission curves showing how the incident solar energy curve gets modified due to passage through different quantities of ozone are given in Fig. 2. Graphical integration of similar absorption curves gave the solar energy aborption for each quantity of ozone, from which a general curve (Fig. 3) was obtained, and this was used for further calculations.

(*b*) *Alternative method.*—Chapman[22] in his paper on "The atmospheric height distribution of band-absorbed solar radiation" suggested that the form

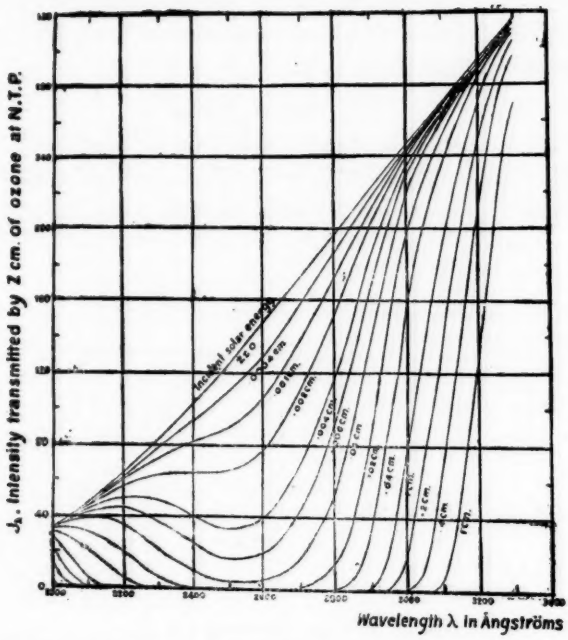

FIG. 2. Intensity of solar radiation in the Hartley band after passage through different thicknesses of ozone in the earth's atmosphere.
Unit of $J_\lambda d\lambda$ = cal. cm.$^{-2}$ sec.$^{-1}$

of the absorption curve can be expressed by the normal error equation:

$$a = a_0 e^{-h^2(\lambda-\lambda_0)^2}, \qquad (1)$$

where a_0 = peak value of a, λ_0 = wavelength corresponding to a_0, and h determines the spread of the band which can be obtained by plotting* log a against $(\lambda - \lambda_0)^2$. Then the fractional absorption at any wavelength λ by Z cm. of ozone will be: $1 - e^{-Z\beta e^{-h^2(\lambda-\lambda_0)^2}}$, where $\beta = 2{\cdot}303\, a_0$. If the solar energy curve in the region between $\lambda_1 = 2000$ Å and $\lambda_2 = 3300$ Å, $(\lambda_1 < \lambda_0 < \lambda_2)$, is assumed to be of the linear form $J_\lambda = k + m\lambda$, the total solar energy absorption by Z cm. of ozone in the band within the limits λ_1 and λ_2 becomes:

* Läuchli and Fabry-Buisson plot log a against λ and give the following empirical formulæ for the region 2800–3350 Å:

$\log a = 17{\cdot}58 - 0{\cdot}0564 \cdot \lambda$ .. .. (F. & B.)
$\log a = 16{\cdot}74 - 0{\cdot}0536 \cdot \lambda$ .. .. (L.)

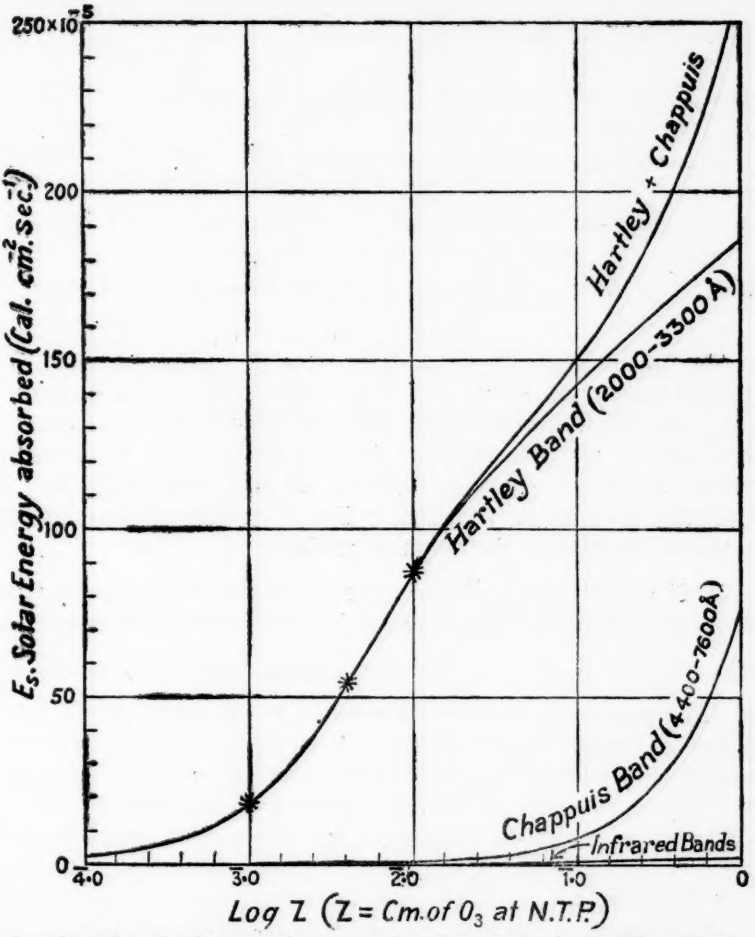

FIG. 3. Absorption of solar energy by Z cm. of ozone at N.T.P. in the different bands.

$$E_s = \int_{\lambda_1}^{\lambda_2} J_\lambda \left(1 - e^{-Z \cdot \beta e^{-k^2(\lambda-\lambda_0)^2}}\right) d\lambda$$

$$= \int_{\lambda_1}^{\lambda_2} (k + m\lambda)\left(1 - e^{-Z \cdot \beta e^{-k^2(\lambda-\lambda_0)^2}}\right) d\lambda.$$

The integral can be evaluated† and shown to be:

† I thank Prof. D. D. Kosambi for his help in the solution. This method for a limited nd can be extended to similar single or composite absorption bands of any gas.—Author.

$$E_s = J_{\lambda_0} \frac{\sqrt{\pi}}{2h} \cdot S_1 + \frac{m}{2h^2} \cdot S_2 \qquad (2)$$

where $S_1 = \sum_1^\infty (-1)^{n+1} \frac{p^n}{n!\sqrt{n}} [\phi(\sqrt{nA}) + \phi(\sqrt{nB})]$,

$S_2 = \sum_1^\infty (-1)^{n+1} \frac{p^n}{n!\,n} [e^{-nA} - e^{-nB}]$,

and $p = \beta Z$, $A = h^2(\lambda_1 - \lambda_0)^2$, $B = h^2(\lambda_2 - \lambda_0)^2$, $J_{\lambda_0} = k + m\lambda_0$,

and ϕ denotes the error function given by $\phi(x) = \frac{2}{\sqrt{\pi}} \int_0^x e^{-t^2}\, dt$.

The infinite series S_1 and S_2 in equation (2) can be evaluated by using tabulated values of $\phi(x)$ and e^{-x}. It is found/that S_1 is the main term, while S_2 is a correction term being the difference of two small and nearly equal quantities. E_s was evaluated for different values of Z of ozone. Three such values (for Z = ·001 cm., ·004 cm., ·01 cm.) are shown by stars on the curve relating to the Hartley band in Fig. 3, showing good agreement with the values obtained by the graphical method.

In Chapman's paper referred to above, he gets the absorption of energy of radiation between wavelengths λ and $\lambda + d\lambda$ between levels m and $m + dm$, which is $\frac{dS_\lambda}{dm}\, d\lambda$, $S_\lambda\, d\lambda$ being the intensity of the incident beam at the level m, and then integrates it over the whole band. In this paper, we do not calculate the density of energy absorption directly, but only the energies absorbed by different finite masses Z cm. of ozone when the incident energy J_λ is of the linear form assumed. The multiplication of the terms J_λ and α_λ (due to differentiation with respect to m) does not therefore appear in our integrals. The actual energy absorption in an atmospheric layer of finite extent will be found by getting the values of the energies absorbed down to the top and base of the layer, beginning at the outer limit of the atmosphere, and then taking their difference. This quantity divided by the mass in the layer gives the mass density of energy absorption. This is an elementary but practical way of getting the density of energy absorption in the different layers of an atmosphere of any arbitrary composition, the values obtained being averages over these regions. This will give equally good results if the layers are taken sufficiently small.

(*c*) It is assumed in accordance with the observations of Vassy[23] that there is no variation of absorption with pressure in the Hartley band. This has been recently verified by Strong.[14]

(*d*) Data by Vassy[24] show that the temperature effect is small and it has been neglected.

(2) *Visible* (*Chappuis*) *Band:* 4400–7600 Å.—This band has been studied by Colange,[26] E. Vassy,[25] A. Tournaire-Vassy[27] in the laboratory, and by Cabannes and Dufay[28] and Fowle[28a] in the atmosphere. Absorption coefficients at 18° C (Fig. 4) from A. Tournaire-Vassy's measurements quoted

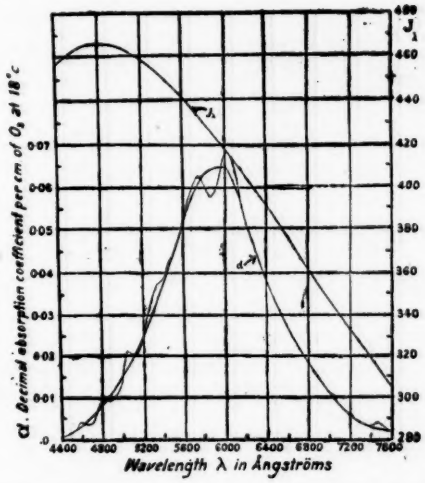

FIG. 4. α, the decimal absorption cofficient per cm. of ozone at N.T.P. in the Chappuis band, and Jλ, the intensity of the incident solar radiation just outside the earth's atmosphere. The coefficients are for a temperature of 18° C, and unit of $J_\lambda d\lambda$ = cal. cm.$^{-2}$ sec.$^{-1}$.

in detail by Götz[29] were used. Since this band lies in a region near the peak of the solar energy curve and is much wider than the Hartley band, it plays a not unimportant part in the absorption of solar energy. Curves similar to those for the Hartley band showing the solar energy absorption by different path lengths of ozone were prepared (Fig. 3).

It will be seen that the Chappuis band becomes important for ozone values higher than about 0·1 cm., *i.e.*, below about 25 km. For places in high latitudes where the sun will be low for many hours, this band will play an important role. This is clearly shown in Fig. 5, which gives the actual solar energy absorption at different levels in the atmosphere for an ozone distribution like that at Tromsø (Lat. 69°40′ N.), for different zenith distances. It is interesting to note that the solar energy absorption curve for the Chappuis band closely follows the ozone distribution curve, since the energy

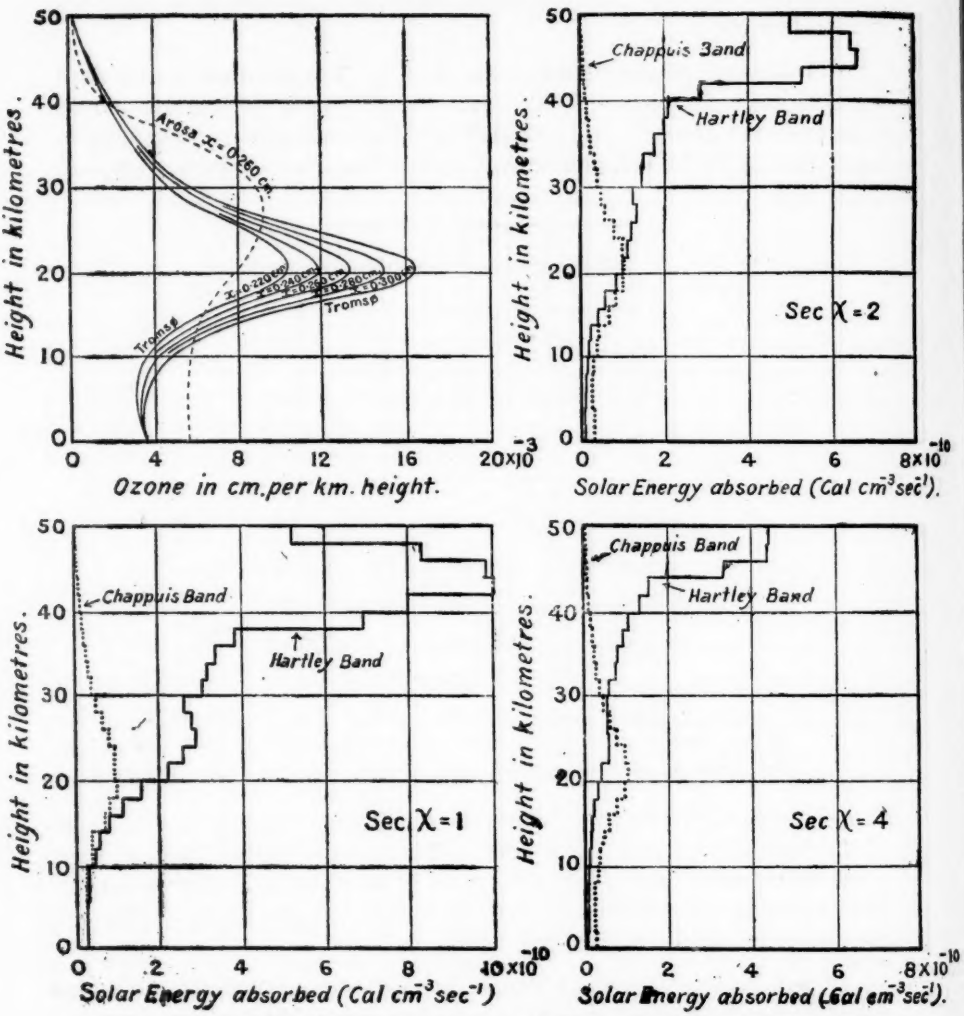

FIG. 5. Vertical distribution of ozone at Tromsø and the corresponding rates of absorption solar energy in the Hartley and Chappuis bands for different zenith distances x of the sun.

absorption varies practically linearly with ozone quantity even up to 1 cm. of ozone.

There are no measurements of the pressure effect on this band. The study of the temperature effect by E. Vassy[25] shows an increase of absorption

coefficient with decrease of temperature, being about 12% greater when the temperature is reduced from 20° C to − 40° C. But the values given are only relative, Colange's value for the maximum absorption coefficient at room temperature being assumed as 0·05. Cabannes and Dufay have also used Colange's values to determine the ozone content of the atmosphere. But the amounts of ozone they have thus obtained seem to be too high, suggesting that the absorption coefficients are too low. Actually in the ozonosphere, lower temperatures than room temperature and hence higher values of the absorption coefficients have to be accepted. The values which are quoted by Götz and used in our calculations are about 36% higher than Colange's values. This is a change on the correct side, though it may not be quantitatively correct. A detailed experimental study with simultaneous observations both in the visible and the ultra-violet regions is still necessary to clarify the matter.

(3) *Infra-red Bands at* 4·75 μ, 9·6 μ and 14·1 μ.—These are comparatively unimportant for the calculation of the absorption of solar energy, since the solar energy curve goes down rapidly in the infra-red. This will be clear from Fig. 3 and Table I which give the solar energy contained in the different ozone bands and the relative absorptions produced by them. Still, the calculations were completed as they are useful for the consideration of the radiation side of the problem.

TABLE I

Intensity of solar radiation $[E_s]_{\lambda_1}^{\lambda_2}$ *in the different ozone bands just outside the earth's atmosphere and the relative absorptions of energy*

Unit of intensity = 10^{-5} cal. cm.$^{-2}$ sec.$^{-1}$

Band	Range	$[E_s]_{\lambda_1}^{\lambda_2}$	Energy absorbed by Z cm. of ozone at N.T.P. when kept at a pressure of 25 mb.			
			Z = ·001 cm.	Z = ·01 cm.	Z = ·1 cm.	Z = 1 cm.
Hartley Band ..	2000–3300 Å	213·5	18·1	86·3	142·5	186·5
Chappuis Band ..	4400–7600 Å	1300·5	0·08	0·81	8·08	77·4
Infra-red 4·75 μ Band	4·65–4·90 μ	2·66	0·04	0·13	0·40	1·19
9·6 μ ,, ..	9·3–10·1 μ	0·58	0·014	0·05	0·14	0·39
14·1 μ ,, ..	12·0–16·5 μ	0·78	0·006	0·02	0·06	0·17
Total for all bands ..		1517·9	18·3	87·3	151·2	265·7

(*a*) For the 9·6 μ band, Adel's [9c] curves on the atmospheric absorption measured at Lowell Observatory were used to calculate the absorption

coefficients (Fig. 6) by a method‡ of reduction and elimination, the effective pressure being taken to be 25 mb., which is roughly the pressure at the centre of gravity of atmospheric ozone. The recent values obtained by

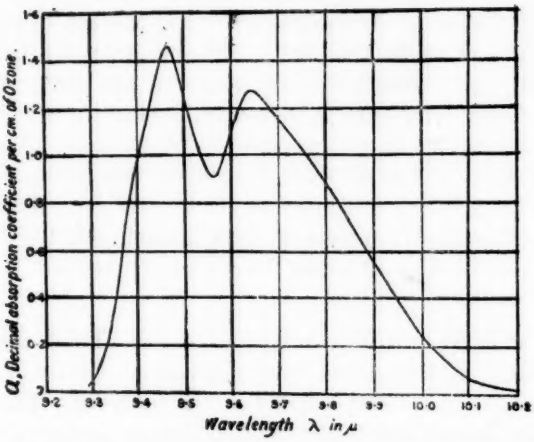

FIG. 6. α, the decimal absorption coefficient per cm. of ozone at N.T.P. in the 9·6 μ infra-red band calculated from the atmospheric measurements of Adel and Lampland.

Strong[14] with the apophyllite residual ray apparatus gave $\alpha = 0{\cdot}8$ to $1{\cdot}0$ per cm. of O_3 at N.T.P. for a gas pressure of 25 mb. and these agree well with those deduced from Adel's data. All old curves gave extremely low values, for example K. Ångström's[30] and Ladenburg and Lehmann's[31] curves gave values of α to be ·005 to ·09 per cm. of ozone, Gerhard's[32] curves gave $\alpha = {\cdot}004$ to ·019, and curves by Hettner and his co-workers[33] gave $\alpha = {\cdot}035$.

(*b*) For the bands at $4{\cdot}75\,\mu$ and $14{\cdot}1\,\mu$, curves recently obtained by Hettner and his co-workers[33] are available. But the quantity of ozone

‡ Out of the different series of observations which Adel gives for the atmospheric transmission in the region $8-11\,\mu$, series A, B and E refer to the same air mass 1·6 but to different water vapour contents, *viz.* 41·5, 21·4 and 3·2 mm. of ppt. H_2O. Detailed knowledge of the absorption due to CO_2 in the same region ($8-11\,\mu$) is available from Barker and Adel's paper (*Phy. Rev.*, Vol. 44, 185, 1933). The total ozone content of the atmosphere was assumed to be the same for the three series, accepting Dobson's mean annual value for the latitude 35° N. of Lowell Observatory as 0·240 cm. at N.T.P. The total CO_2 content was also taken to be the same for the three series, accepting the value 240 cm. at N.T.P. This enabled the effects due to water vapour, CO_2 and ozone to be separated, so that by eliminating the effects of water vapour and CO_2, the absorption due to ozone alone could be calculated at each wavelength. Fig. 6 gives the mean decimal absorption coefficient α obtained from the three series, the effective gas pressure being taken to be 25 mb. which is the pressure at the centre of gravity o atmospheric ozone.

mentioned by these authors (30 cm. of 'practically pure' ozone under a pressure of 160 mm. of mercury) seems to be too high. If the values of the absorption coefficients obtained from Adel's and Strong's observations at $9{\cdot}6\,\mu$ are taken to be correct and Strong's empirical fourth root law for pressure effect is adopted, this quantity would completely black out most of the $9{\cdot}6\,\mu$ band. Hettner's curves however show as much as 5% transmission at the peak of the band. Elsasser[7e] also in his paper expresses a doubt about this, but disposes of the matter by saying that the true amount may be different owing to the fact that the line-broadening effect of ozone upon itself may be different from that of air upon ozone. But this is only a speculation. According to Hertz,[34] Eva Bahr[35] and others the line-broadening effect due to the addition of air or of the pure gas obeys the square root law in the case of CO_2 and water vapour. The only available laboratory data in the case of ozone are those by Strong who proposes the fourth root law. But whichever law is nearer the truth, it is difficult to accept the quantity mentioned by Hettner and his co-workers. The best way seems to be to accept Adel's results as correct for the $9{\cdot}6\,\mu$ band and recalculate the partial pressures of ozone in the experiments of Hettner, and thence the absorption coefficients in the other regions. The average absorption coefficients k given in the appendix are obtained in this manner, using Elsasser's relation $A = \phi(\sqrt{kZ})$, and the fourth root law proposed by Strong to take into account the pressure effect.

(*c*) Though Strong has proposed the fourth root law for the pressure effect, most other workers propose the square root law for the infra-red region in general. It is difficult to see why the $9{\cdot}6\,\mu$ band of ozone should be an exception to the square root law. The use of the apophyllite residual ray apparatus in Strong's observations necessarily involves the reflection contour characteristic of the material used, and what is obtained is the combined integrated effect of the reflection contour and ozone absorption. Results obtained with such apparatus are therefore not strictly comparable with those with sufficient spectral details. The use of any higher root law only means less variation of absorption with pressure. For the use of any nth root law in this connection, coefficients appropriate to a standard pressure p_0 are to be calculated from observations made at any pressure p on a quantity Z cm. of ozone, using the relation $Z\sqrt[n]{\frac{p}{p_0}}$. For calculations in the ozone bands, the standard pressure p_0 is taken to be 25 mb., which is roughly the pressure at the centre of gravity of ozone. It was also arbitrarily decided to accept the fourth root law for all infra-red bands of ozone, since no other results than those of Strong are available for the pressure effect. For carbon

dioxide and water vapour bands, however, the square root law was used in accordance with the conclusions of Hertz and Eva Bahr. It was seen (Fig. 3) that the actual value of the solar energy absorbed by ozone in all the infra-red bands taken together becomes very small as compared with the absorption of energy in the ultra-violet and the visible regions, and hence it matters very little whether the square root law or the fourth root law is used to take account of the pressure effect.

(*d*) The temperature effect was neglected due to lack of available data. In any case, the total absorption being small, the neglect is not important.

§ 4. Carbon Dioxide Bands

All CO_2 bands lie in the infra-red region beyond 2 μ. Still the total CO_2 content of the atmosphere being as large as 240 cm. at N.T.P., it plays a part in the absorption of solar energy, especially in the lower stratosphere.

The important bands are at 2·7 μ, 4·3 μ, 9–11 μ and 12·5–17·5 μ. For the 2·7 μ band, Barker's[36] curve was used. Absorption curves for different quantities of CO_2 were prepared similar to those for ozone, using Beer's law for each wavelength ; graphical integration of such curves gave the solar energy absorption for the band. For the 4·3 μ band, Martin and Barker's [11] new curves were used. For the remaining two bands, data collected

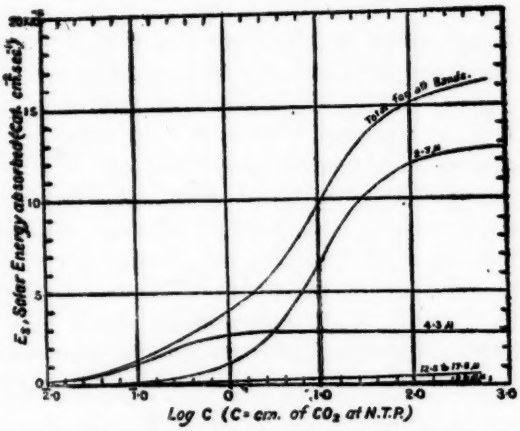

Fig. 7. Absorption of solar energy by C cm. of CO_2 at N.T.P. in the different bands.

by Callendar[13] were used, adopting his empirical formula $A = 1 - (1 + nc^x)^{-1}$. The comparative importance of the different CO_2 bands for the absorption of solar energy will be seen from Fig. 7 and Table II.

TABLE II

Intensity of solar radiation $[E_s]_{\lambda_1}^{\lambda_2}$ *in the different* CO_2 *bands just outside the earth's atmosphere and the relative absorptions of energy*

Unit of intensity = 10^{-5} cal. cm.$^{-2}$ sec.$^{-1}$

Band	$[E_s]_{\lambda_1}^{\lambda_2}$	Energy absorbed by C cm. of CO_2 at N.T.P.					
		C = ·01cm.	C = ·1 cm.	C = 1 cm.	C = 20 cm.	C = 100 cm.	C = 240 cm.
2·66–2·82 μ	12·76	·01	0·11	1·07	9·00	11·76	12·38
4·19–4·37 μ	2·87	·15	1·15	2·76	2·87	2·87	2·87
9–11 μ	1·33	0	0	0	0·01	0·02	0·05
12·5–17·5 μ	0·72	·01	0·04	0·15	0·36	0·46	0·51
Total for all bands	17·68	0·17	1·30	3·98	12·24	15·11	15·81

The square root law was used for the pressure effect and the temperature variation of absorption coefficients was neglected.

It is to be noted that the last two bands partly overlap the corresponding ozone bands, while the first two and also the last overlap the corresponding water vapour bands. Absorptions due to the different absorbents in a common band will be additive as long as each is only a few per cent. For large absorptions, however, the transmissions will be multiplicative. This has to be taken into consideration when actually evaluating the energy absorptions due to a given distribution of the absorbents.

§ 5. WATER VAPOUR BANDS

Absorption due to water vapour begins in the near infra-red at about 0·9 μ and extends with varying intensity throughout the infra-red region with a transparent window between 8 and 11 μ. Though the maximum amount of water vapour present above the tropopause may not exceed 0·03 cm. of precipitable water, the region of absorption is so extensive and some of the bands in the region 2 to 8 μ so intense that even this small quantity contributes an important share to the solar energy absorption. The main bands up to 8 μ are shown in Table III.

Complete spectroscopic observations with very small amounts of water vapour such as may be present in the upper atmosphere are not available. The lowest quantity for which Fowle[37] gives data is 0·008 cm. of precipitable water, while Hettner's[38] data in this region were obtained for about 0·06 cm. of precipitable water. There is general agreement between the values

TABLE III

Intensity of solar radiation $[E_s]_{\lambda_1}^{\lambda_2}$ *in the different water vapour bands just outside the earth's atmosphere and the relative absorptions of energy in the region* $0{\cdot}9\,\mu$ *to* $8\,\mu$

Unit of intensity $= 10^{-5}$ cal. cm.$^{-2}$ sec.$^{-1}$

Author	Band	Range in μ	$[E_s]_{\lambda_1}^{\lambda_2}$	Energy absorbed by W cm. of ppt. H_2O			
				W = ·0001 cm.	W = ·001 cm.	W = ·008 cm.	W = ·04 cm.
Hettner	ρ	0·89–0·99	200·8	0·01	0·13	1·01	5·00
	ϕ	1·08–1·19	139·4	0·02	0·17	1·36	6·68
	ψ	1·27–1·53	185·1	0·15	1·41	10·55	42·78
	Ω	1·70–2·02	95·0	0·09	1·07	7·99	29·66
Fowle	x_1	2·2–3·2	91·5	2·45	7·74	21·60	45·58
	x_2	3·2–4·0	24·9	0·61	1·93	5·40	11·50
	Y	4·0–4·9	12·8	0·48	1·50	4·15	8·32
	Z*	4·9–8·0	12·6	0·62	1·95	5·08	8·68
Total for all bands			762·1	4·43	15·90	57·14	158·20

* Calculations were made separately for the component bands Z_1 (4·9—5·4 μ), Z_2 (5·4—5·9 μ), Z_3 (5·9—6·4 μ), Z_4 (6·4—7·0 μ) and Z_5 (7·0—8·0 μ) as mentioned by Fowle and added up.

obtained from the two measurements only in the region up to $2\,\mu$ and for small values of precipitable water. For the range 2 to $8\,\mu$, where the absorption is so large as to blackout the band heads in Hettner's observations, the results obtained by the two authors are not comparable and Fowle's data have been used.

In a recent paper, Fox and Martin[39] have investigated the absorption spectrum of water in the three states and in solution in carbon tetrachloride in the region 2·5–7·5 μ. They have however explored the spectrum of *water vapour* only in the region 2·5 to 2·85 μ. From the molecular extinction coefficients they have presented, it seems that the limits of the band are narrower than those given by Fowle, or the wings of the bands are too weak for detailed measurements. Calculations for the same quantity of precipitable water (W = ·008 cm.) which Fowle had used show that the average absorption over the region 2·5 to 2·85 μ is 45·6%, whereas over the region 2·2 to 3·2 μ it becomes 15·3%. The latter value may be compared with Fowle's figure 23·6% for the same region. Fowle's figure has been used in our calculations.

Another interesting point mentioned by Fox and Martin is that the 4·7 μ band found in the solid and liquid states of water has no counterpart

in the vapour spectrum and has therefore been attributed by them to associated water molecules. On the other hand, Fowle's curves for W = ·008 cm. of precipitable water show as much as 30% absorption in this region, and this cannot be attributed to CO_2, as there is no CO_2 band at 4·7 μ. In any case, from the point of view of our present calculations of the solar energy absorption, this does not affect our general conclusions seriously.

For the region 0·9 μ to 2 μ, Hettner's curves giving more spectral details were reduced in a way similar to that used for the Hartley band of ozone, and the energy absorption was obtained by graphical integration. Beyond 2 μ, Fowle's results were used, Elsasser's error function being applied over the subregions to get the energy absorptions due to different quantities of water vapour. Table III and Fig. 8 summarise the results. It is to be noted that in the first region up to 2 μ, the absorption is weak though the solar energy

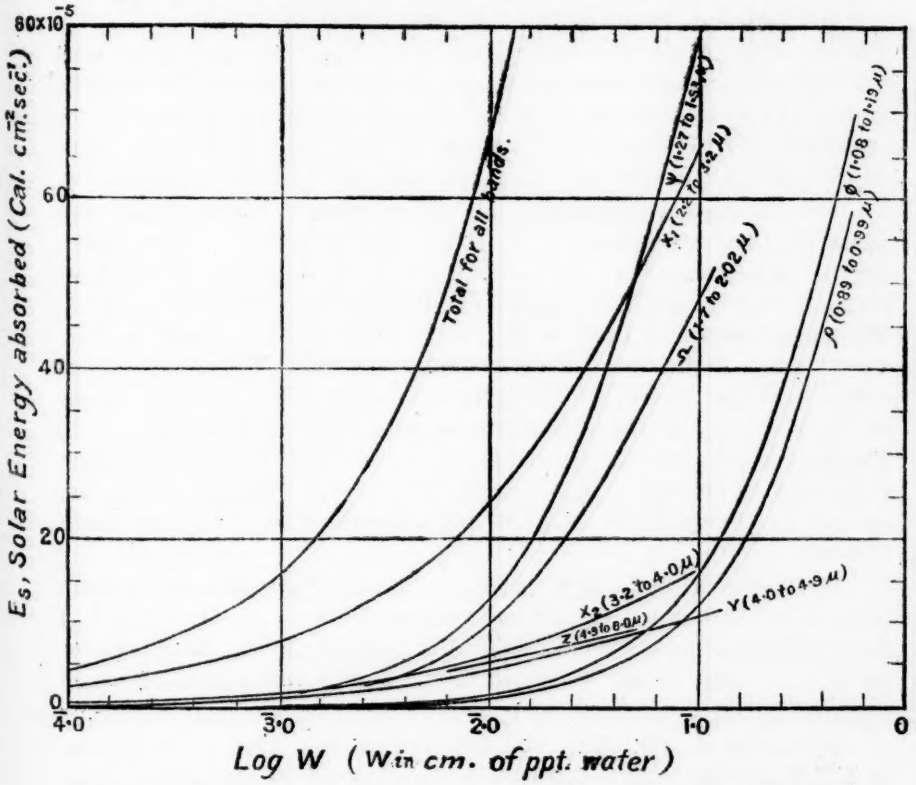

FIG. 8. Absorption of solar energy by W cm. of precipitable water in the different bands.

is large, whereas in the second region the energy is small but the strong absorption takes away most of the energy. The bands in the second region are therefore effective in the uppermost layers of the atmosphere.

The temperature effect is negligible for the values of water vapour involved in the upper atmosphere, as indicated by Elsasser[7c] and Cowling.[8] For the pressure effect, the square root law was used as for carbon dioxide.

§ 6. Height-Distribution of the Constituents and the Calculation of Solar Energy Absorption

(*a*) *Ozone.*—The vertical distribution of atmospheric ozone has been investigated for the following places:—

(i) At Arosa[2a] in Switzerland.

(ii) At Tromsø.[2b]

(iii) At Stuttgart in Germany by Regener.[3]

(iv) In U.S.A. by the Bureau of Standards[4] and Explorer II.

For the study of the solar energy absorption, the first two cases were selected; the remaining cases can be treated in a similar way. The difficulty common to all of them lies in the fact that the distribution of ozone in the uppermost layers (above 40 km.) is not known with sufficient accuracy, while ozone quantities at these levels are important for solar energy absorption.

For the present calculations, the ozone content above 50 km. was neglected. The atmosphere up to 50 km. was divided into 2 km. layers, and the ozone content in each layer and also down to the base of each layer obtained graphically. The temperature effect on absorption was neglected. The energy absorption down to the base of each layer was found by using curves similar to the curves of Fig. 3 on a linear scale. The energy absorption in each layer was obtained by differences and this divided by the volume of the air in the layer gives the volume density of energy absorption, E_v. The mass density of energy absorption, E_m, is given by dividing the absorption in the layer by the mass of air traversed. For a zenith distance χ of the sun, the rate of absorption of energy in any atmospheric layer is proportional to cos χ.

Fig. 9 gives the values of E_v and E_m for the ozone distribution at Tromsø (total $0_3 = 0{\cdot}260$ cm.). Calculations were made for sec $\chi = 1, 1{\cdot}5, 2, 3, 4$ for averaging the results afterwards for the whole of the day, but curves for sec $\chi = 1, 2$ and 4 only are shown here. Similar curves have also been prepared for the distribution at Arosa.

(*b*) *Carbon dioxide.*—The total CO_2 content was taken to be 240 cm. at N.T.P. and the vertical distribution was obtained by assuming it to be present throughout the lower 50 km. in the same proportion of the total air

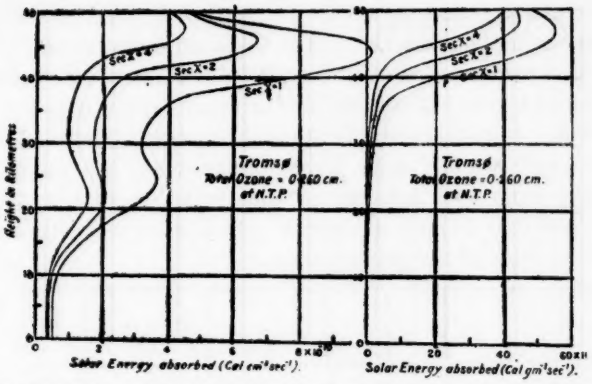

FIG. 9. Height distribution of the absorption of solar energy by ozone at Tromsø. Total ozone, $x = 0{\cdot}260$ cm. at N.T.P.

as at the surface. To get the equivalent quantities for absorption, the amount in each layer was multiplied by $\sqrt{\frac{p}{p_0}}$, adopting the pressure distribution in the atmosphere recently given by Penndorf.[40] Temperature effect was neglected. Curves similar to the curves of Fig. 7 on a linear scale were used to find the energy absorption due to different values of CO_2. Fig. 10

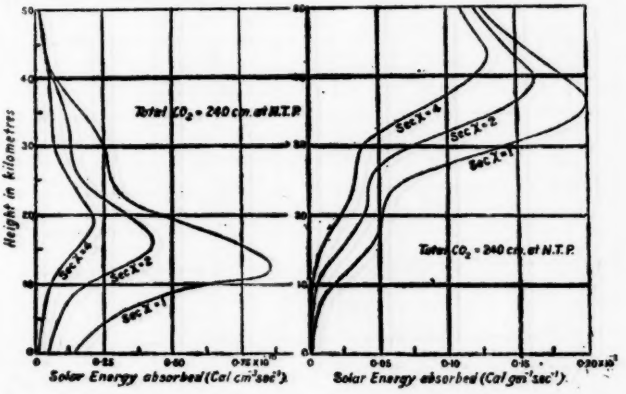
Height in kilometres
Total CO₂ = 240 cm. at N.T.P.
Sec X = 4
Sec X = 2
Sec X = 1
Solar Energy absorbed (Cal cm⁻² sec⁻¹).
Solar Energy absorbed (Cal gm⁻² sec⁻¹).

FIG. 10. Height distribution of the absorption of solar energy by carbon dioxide. Total CO_2 content of the atmosphere $=240$ cm. at N.T.P. and CO_2 assumed to exist in the same proportion at all heights.

gives the absorption of solar energy by CO_2 for three different zenith distances of the sun.

(*c*) *Water vapour.*—No ' measurements ' of the amount and distribution of water vapour in the stratosphere are available. Simpson[41] considered

that the stratosphere contained about 0·3 mm. of precipitable water. This was based on the assumption that the air was saturated at the base of the stratosphere at a temperature of about 220° A. Ramanathan[42] pointed out that in the tropics at any rate, the amount of water vapour in the stratosphere should be much less because of the much lower temperatures at the tropopause. Brunt and Kapur[43] have given tables with the values of water content ranging from 0·01 mm. at the equator to 0·1 mm. in the latitude 50° in winter and to 0·17 mm. in summer. In a later paper, Brunt[44] regards these as overestimates of the actual values.

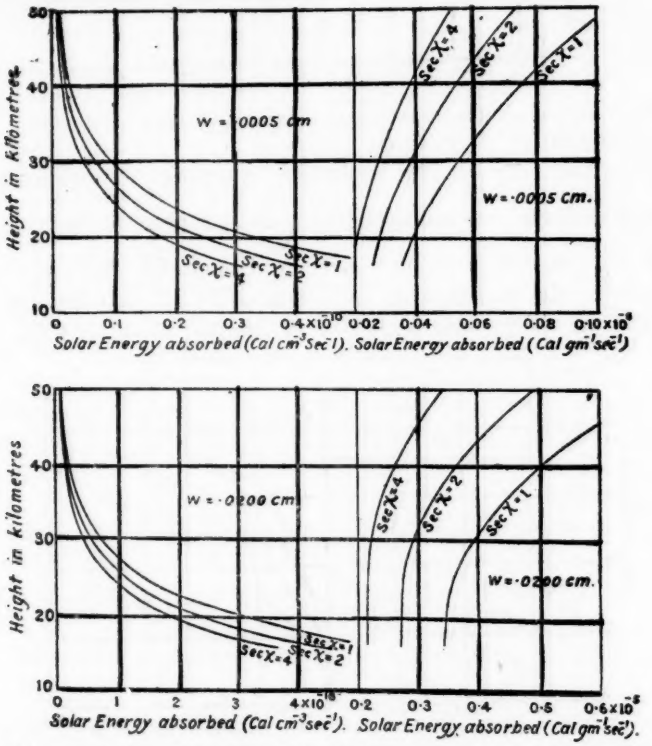
Height in Kilometres
W = ·0005 cm
Sec χ = 4
Sec χ = 2
Sec χ = 1
W = ·0005 cm.
Solar Energy absorbed (Cal cm⁻³ Sec⁻¹). Solar Energy absorbed (Cal gm⁻¹ sec⁻¹)
Height in kilometres
W = ·0200 cm
W = ·0200 cm.
Solar Energy absorbed (Cal cm⁻³ sec⁻¹). Solar Energy absorbed (Cal gm⁻¹ sec⁻¹).

FIG. 11. Height distribution of the absorption of solar energy by water vapour. W=total precipitable water above 16 km. Relative humidity near 16 km. is assumed to be 100% and the distribution of moisture in the stratosphere governed by Dalton's law.

Recent measurements in Europe show that the stratosphere there is often surprisingly dry, dew points as low as − 80° C being obtained. In the present paper, calculations are made for four different values of total precipitable water above the arbitrarily chosen reference level of 16 km., W = ·0005.

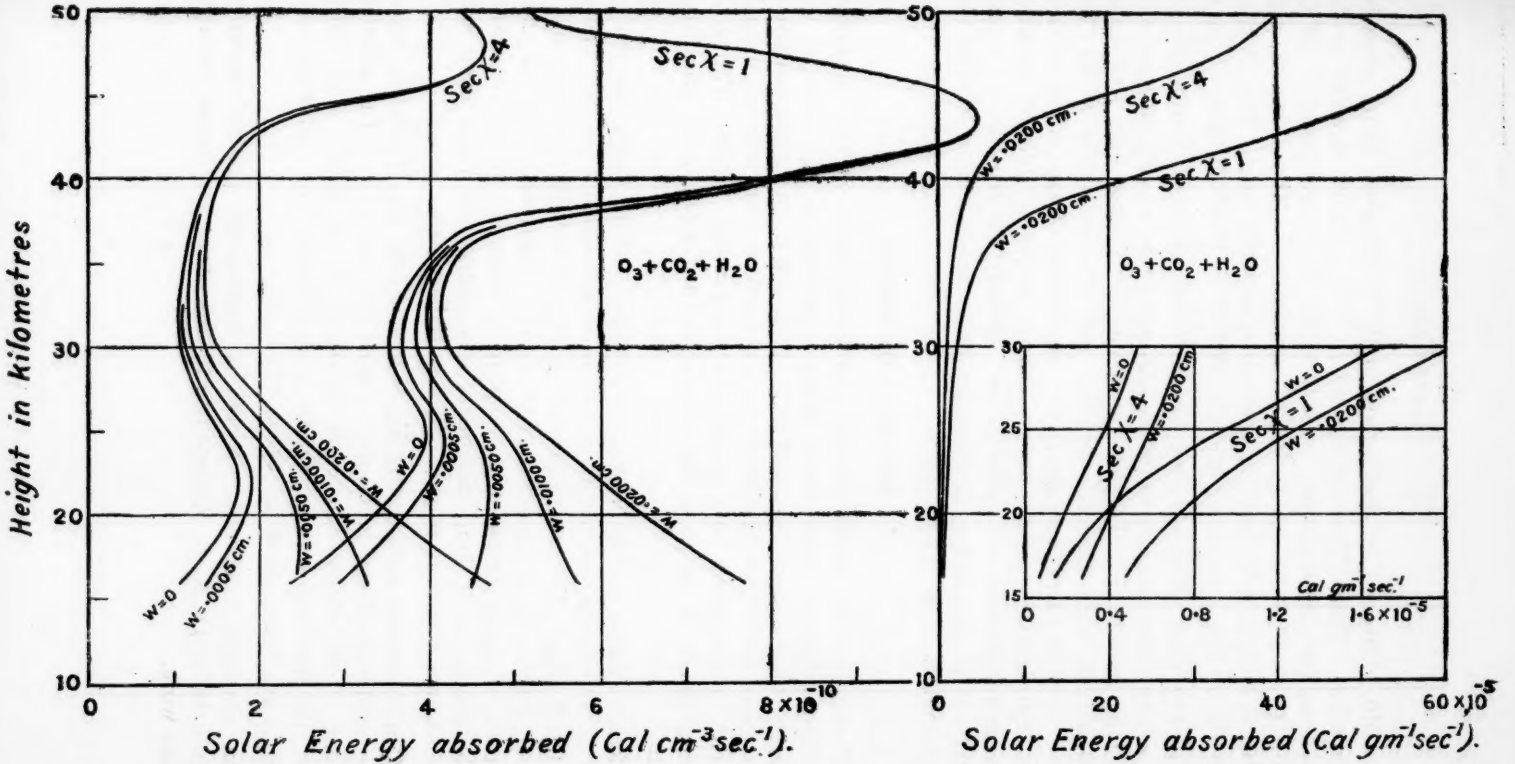
Height in kilometres
Sec χ = 4
Sec χ = 1
O3 + CO2 + H2O
W = 0
W = ·0005 cm.
W = ·0050 cm.
W = ·0100 cm.
W = ·0200 cm.
Solar Energy absorbed (Cal cm-3 sec-1).
Solar Energy absorbed (Cal gm-1 sec-1).
Cal gm-1 sec-1

FIG. 12. Height distribution of the absorption of solar energy by (i) ozone (distribution at Tromsø for $x = 0{\cdot}260$ cm.) plus (ii) carbon dioxide (total CO_2 content = 240 cm.), plus (iii) water vapour (total ppt. H_2O above 16 km. =W cm.). Inset on the right-hand side gives the values of E_m below 30 km. on a magnified scale.

·005, ·010, ·020 cm., the distribution in the stratosphere being given by Dalton's law. These values correspond to 100% relative humidity at the tropopause, the approximate saturation temperatures being $-80°$ C, $-65·5°$ C, $-60·5°$ C and $-55·5°$ C respectively. These results with suitable changes may be used for application to actual cases. Fig. 11 gives the results for the two extreme values of W and for different values of sec χ.

(*d*) *The total effect.*—Having obtained the separate contributions to solar energy absorption due to ozone, CO_2 and water vapour, the three may be suitably added. Fig. 12 gives the results for Tromsø with total ozone $x = 0·260$ cm., total CO_2 C = 240 cm., and different values of W. The mass density of energy absorption for ozone near 50 km. is considerably larger than that due to water vapour and the curves for different values of W merge into each other. Below 30 km., however, the two effects are comparable and the inset in Fig. 12 shows the results on an enlarged scale for two extreme values of W.

§ 7. Discussion of Results

Throughout the work, the calculations are made on the assumption that the quantity of ozone above 50 km. is negligible. The effect of this will be to reduce slightly the actual values of E_v and E_m in the first few layers. But as stated by Dobson, the ozone values above 45 km. are only approximate and one cannot expect very accurate results for this region. The error decreases rapidly as we go to the lower layers, and is practically zero below 40 km.

Results similar to Fig. 9 were obtained also for the ozone distribution at Arosa and the general nature of the curves was found to be the same as that for Tromsø. The energy absorption near 50 km. level is large and it goes on decreasing as we approach the earth. This means that the small quantities of ozone present in the uppermost layers are mainly responsible for the absorption of large amounts of solar energy, the main ozone mass near its centre of gravity playing only a subsidiary part.

Considering the mass density E_m of solar energy absorption, the region under consideration can be roughly divided into two parts. The contribution due to ozone predominates in the region 50 to 30 km., while below 30 km., the effect due to water vapour predominates. The contribution due to CO_2 is small throughout the region.

In conclusion, the author wishes to express his grateful thanks to Diwan Bahadur Dr. K. R. Ramanathan for his advice and interest throughout this work.

APPENDIX I

Values of the Absorption Coefficients and Other Constants Used in this Paper

(1) *Radiation and solar constants.*—

$C_1 = 3{\cdot}703 \times 10^{-5}$ erg cm.$^{-2}$ sec.$^{-1}$; $C_2 = 1{\cdot}433$ cm. °K.;

$\sigma = 5{\cdot}709 \times 10^{-5}$ erg cm.$^{-2}$ sec.$^{-1}$ K.$^{-4}$;

1 erg cm.$^{-2}$ sec.$^{-1}$ $= 2{\cdot}389 \times 10^{-8}$ cal. cm.$^{-2}$ sec.$^{-1}$

Solar Constant, S $= 2{\cdot}045$ cal. cm.$^{-2}$ min.$^{-1}$

For the distribution of radiant energy, the temperature of the sun is assumed to be 6000° K.

(2) *Ozone bands.*—

α = decimal absorption coefficient per cm. of ozone measured at N.T.P. Only a few values of α read from the smoothed curves are given.

k = generalized absorption coefficient per cm. of ozone in the relation $A = \phi(\sqrt{kZ})$.

Author	Ny Tsi-Ze and Choong		A. Tournaire—Vassy		Adel and Lampland		Hettner, Pohlmann and Schumacher	
Band	Hartley 2000–3300 Å		Chappuis 4400–7600 Å		9·6 μ		4·75 μ	14·1 μ
Pressure	Atmospheric		Atmospheric		25 mb.		25 mb.	25 mb.
	λ in Å	α	λ in Å	α at 18° C	λ in μ	α	Average k	Average k
	2000	(1)	4400	·001	9·3	·04		
	2200	25	4800	·008	9·4	·99		(*a*) Average for 12–13μ and 15·2–16·5μ, k = ·0115
	2400	99·2	5200	·025	9·46	1·45		
	2500	139	5600	·052	9·5	1·27	Average for the region 4·65–4·90μ, k=0·177	
	2553	145	6000	·065	9·56	·91		
	2600	138·5	6400	·038	9·6	1·11		(*b*) Average for 13–15·2μ, k = ·093
	2700	97·5	6800	·018	9·65	1·27		
	2900	19·8	7200	·005	9·7	1·15		
	3100	1·47	7600	·002	9·9	·54		
	3300	·065	..	..	10·1	·06		

(3) *Carbon dioxide bands.*—(*a*) α = decimal absorption coefficient per cm. of CO_2 at N.T.P.

Barker, 1922.				Martin and Barker, 1932.
2·7 μ band				4·3 μ band
λ in μ	α	λ in μ	α	Average α
2·667	·017	2·753	·073	(*a*) For 4·19 to 4·21 μ, α = 0·97
2·677	·089	2·767	·025	(*b*) For 4·21 to 4·30 μ, α = 3·57
2·691	·031	2·777	·062	(*c*) For 4·30 to 4·37 μ, α = 1·18
2·698	·089	2·80	·013	(*d*) Average for 4·19 to 4·37μ, α = 2·10
2·733	·011	2·81	·003	..

(*b*) Callendar's empirical formula for CO_2 bands: $A = 1 - (1 + nc^x)^{-1}$, where C = cm. of CO_2 at N.T.P.

Band	14–16 μ	13–14 μ and 16–17 μ	12·5–13 μ and 17–17·5 μ	9–11 μ
n ..	0·9	0·08	0·0055	0·00017
x ..	0·84	0·67	0·67	1

(4) *Water vapour bands.*—(*a*) Hettner's data used: α = decimal absorption coefficient per cm. of ppt. H_2O at N.T.P.

ρ (0·89–0·99 μ)	ϕ (1·08–1·19 μ)	ψ (1·27–1·53 μ)		Ω (1·70–2·02 μ)	
Average α	Average α	λ in μ	α	λ in μ	α
0·274	0·533	1·27	0	1·70	0
		1·30	0·55	1·75	0·43
		1·33	2·38	1·78	2·19
		1·35	6·50	1·80	5·15
		1·37	10·1	1·82	9·90
		1·40	6·89	1·86	12·6
		1·43	3·77	1·90	10·1
		1·45	1·88	1·94	5·46
		1·49	0·73	1·96	2·23
		1·53	0	2·00	0·37
		..	..	2·02	0·16

(*b*) Fowle's data for W = 0·008 cm. of ppt. H_2O was used to calculate β in the relation $A = \phi(\sqrt{\beta W})$.

Band	Range in μ	Observed % absorption	β
X_1 ..	2·2–3·2	23·6	5·6
X_2 ..	3·2–4·0	21·7	4·7
Y ..	4·0–4·9	32·5	11·0
Z_1 ..	4·9–5·4	18	3·2
Z_2 ..	5·4–5·9	47	24·7
Z_3 ..	5·9–6·4	64	52·4
Z_4 ..	6·4–7·0	68	61·8
Z_5 ..	7·0–8·0	25	6·3

APPENDIX II

Evaluation of the Band-Absorption of Radiation

The band absorption of radiation incident on a gaseous layer of thickness Z can be evaluated as follows, when the relation between the decimal absorption coefficient a and the wavelength λ has the form of the normal error equation, $a = a_0 e^{-h^2(\lambda-\lambda_0)^2}$, and the intensity of the incident radiation has the linear form $J_\lambda = k + m\lambda$. The energy absorption in the band within the limits λ_1 to λ_2, $(\lambda_1 < \lambda_0 < \lambda_2)$, is

$$E_s = \int_{\lambda_1}^{\lambda_2} J_\lambda \,(1 - e^{-Z\beta e^{-h^2(\lambda-\lambda_0)^2}})\, d\lambda, \text{ where } \beta = 2{\cdot}303\, a_0$$

$$= \int_{\lambda_1-\lambda_0}^{\lambda_2-\lambda_0} [k + m\,(u+\lambda_0)]\,(1 - e^{-Z\beta e^{-h^2u^2}})\, du, \text{ by putting } \lambda - \lambda_0 = u$$

$$= (k + m\lambda_0) \int_{\lambda_1-\lambda_0}^{\lambda_2-\lambda_0} (1 - e^{-\beta Z e^{-h^2u^2}})\, du + m \int_{\lambda_1-\lambda_0}^{\lambda_2-\lambda_0} u\,(1 - e^{-\beta Z e^{-h^2u^2}})\, du.$$

Putting $p = \beta Z$ and $x = \beta Z e^{-h^2u^2} = p e^{-h^2u^2}$,

clearly $1 - e^{-\beta Z e^{-h^2u^2}} = 1 - e^{-x} = \sum_1^\infty (-1)^{n+1} \frac{x^n}{n!} = \sum_1^\infty (-1)^{n+1} \frac{p^n}{n!}\, e^{-nh^2u^2}$.

$$\therefore\quad E_s = (k + m\lambda_0) \int_{\lambda_1-\lambda_0}^{\lambda_2-\lambda_0} \left(\sum_1^\infty (-1)^{n+1} \frac{p^n}{n!}\, e^{-nh^2u^2}\right) du$$

$$+ m \int_{\lambda_1-\lambda_0}^{\lambda_2-\lambda_0} \left(\sum_1^\infty (-1)^{n+1} \frac{p^n}{n!}\, u\, e^{-nh^2u^2}\right) du.$$

$$= (k + m\lambda_0)\, I_1 + m\, I_2.$$

The integrals I_1 and I_2 involving infinite series can be solved term by term as follows:—

$$I_1 = \int_{\sqrt{n}\,h\,(\lambda_1-\lambda_0)}^{\sqrt{n}\,h\,(\lambda_2-\lambda_0)} \sum_1^\infty (-1)^{n+1} \frac{p^n}{n!} \cdot \frac{1}{\sqrt{n}\,h}\, e^{-t^2}\, dt \text{ by putting } \sqrt{n}\,hu = t,$$

$$= \sum_1^\infty (-1)^{n+1} \frac{p^n}{n!} \cdot \frac{1}{\sqrt{n}\,h} \cdot \frac{\sqrt{\pi}}{2} \frac{2}{\sqrt{\pi}} \int_{\sqrt{n}\,h\,(\lambda_1-\lambda_0)}^{\sqrt{n}\,h\,(\lambda_2-\lambda_0)} e^{-t^2}\, dt$$

$$= \sum_1^\infty (-1)^{n+1} \frac{p^n}{n!} \frac{\sqrt{\pi}}{2\sqrt{n}\,h} \left[\frac{2}{\sqrt{\pi}} \int_{\sqrt{n}\,h\,(\lambda_1-\lambda_0)}^{0} e^{-t^2}\, dt + \frac{2}{\sqrt{\pi}} \int_0^{\sqrt{n}\,h\,(\lambda_2-\lambda_0)} e^{-t^2}\, dt\right]$$

since $\lambda_1 < \lambda_0 < \lambda_2$, *i.e.*, $\lambda_1 - \lambda_0 < 0 < \lambda_2 - \lambda_0$.

$$= \sum_1^\infty (-1)^{n+1} \frac{p^n}{n!} \frac{\sqrt{\pi}}{2\sqrt{n}\,h} \left[\frac{2}{\sqrt{\pi}} \int_0^{\sqrt{n}\,h\,(\lambda_0 - \lambda_1)} e^{-t^2}\,dt + \frac{2}{\sqrt{\pi}} \int_0^{\sqrt{n}\,h\,(\lambda_2 - \lambda_0)} e^{-t^2}\,dt \right]$$

$$= \sum_1^\infty (-1)^{n+1} \frac{p^n}{n!} \frac{\sqrt{\pi}}{2\sqrt{n}\,h} \left[\phi\left(\sqrt{n}\,h\,\overline{\lambda_0 - \lambda_1}\right) + \phi\left(\sqrt{n}\,h\,\overline{\lambda_2 - \lambda_0}\right) \right]$$

where ϕ denotes the well-known error function.

$$\text{Also, } I_2 = \int_{\lambda_1 - \lambda_0}^{\lambda_2 - \lambda_0} \sum_1^\infty (-1)^{n+1} \frac{p^n}{n!}\, u\, e^{-nh^2u^2}\,du$$

$$= \int_{nh^2(\lambda_1 - \lambda_0)^2}^{nh^2(\lambda_2 - \lambda_0)^2} \sum_1^\infty (-1)^{n+1} \frac{p^n}{n!} \cdot \frac{1}{2nh^2}\, e^{-y}\,dy \ \ldots\ldots \text{ by putting } nh^2u^2 = y$$

$$= \sum_1^\infty (-1)^{n+1} \frac{p^n}{n!} \cdot \frac{1}{2nh^2} \left[\frac{e^{-y}}{-1} \right]_{nh^2(\lambda_1 - \lambda_0)^2}^{nh^2(\lambda_2 - \lambda_0)^2}$$

$$= \sum_1^\infty (-1)^{n+1} \frac{p^n}{n!} \cdot \frac{1}{2nh^2} \left[e^{-nh^2(\lambda_1 - \lambda_0)^2} - e^{-nh^2(\lambda_2 - \lambda_0)^2} \right]$$

$$\therefore\ E_s = (k + m\lambda_0) \frac{\sqrt{\pi}}{2h} \sum_1^\infty (-1)^{n+1} \frac{p^n}{n!\sqrt{n}} \left[\phi\left(\sqrt{nh^2(\lambda_0 - \lambda_1)^2}\right) + \phi\left(\sqrt{nh^2(\lambda_2 - \lambda_0)^2}\right) \right]$$

$$+ \frac{m}{2h^2} \sum_1^\infty (-1)^{n+1} \frac{p^n}{n!\,n} \left[e^{-nh^2(\lambda_1 - \lambda_0)^2} - e^{-nh^2(\lambda_2 - \lambda_0)^2} \right]$$

Putting $h^2(\lambda_1 - \lambda_0)^2 = A$, $h^2(\lambda_2 - \lambda_0)^2 = B$, and $k + m\lambda_0 = J_{\lambda 0}$,

$$E_s = J_{\lambda_0} \frac{\sqrt{\pi}}{2h} \sum_1^\infty (-1)^{n+1} \frac{p^n}{n!\sqrt{n}} \left[\phi\left(\sqrt{nA}\right) + \phi\left(\sqrt{nB}\right) \right]$$

$$+ \frac{m}{2h^2} \sum_1^\infty (-1)^{n+1} \frac{p^n}{n!\,n} \left[e^{-nA} - e^{-nB} \right]$$

$$= J_{\lambda 0} \frac{\sqrt{\pi}}{2h} \cdot S_1 + \frac{m}{2h^2} \cdot S_2$$

REFERENCES

1. Gowan .. (*a*) *Proc. Roy. Soc. A*, 1928, **120**, 655.
   .. (*b*) *Ibid.*, 1930, **128**, 531.
2. (*a*) Götz, Meetham and Dobson *Proc. Roy. Soc. A*, 1934, **145**, 416.
   (*b*) Meetham and Dobson .. *Ibid.*, 1935, **148**, 598.
3. (*a*) E. & V. H. Regener .. *Physik. Z.*, 1934, 35, 788.
   (*b*) V. H. Regener .. *Naturwiss.*, 1938, **26**, 155.
   (*c*) V. H. Regener .. *Zeit. fur Physik*, 1938, **109**, 642.
4. Coblentz and Stair .. *Jr. of Res. Nat. Bur. Std.*, 1938, **20**, 185 : 1939, **22**, 295 ; 1939, **22**, 573 ; 1941, **26**, 161.
   Coblentz and Stair .. *Mon. Wea. Rev.*, 1939, **67**, 331.
5. Penndorf .. *Veröff. Geophys. Inst. Leipzig*, 1936, **8**, 181–285.
6. Godfrey and Price .. *Proc. Roy. Soc. A*, 1937, **163**, 228.
7. W. M. Elsasser .. (*a*) *Astrophy. Jour.*, 1938, 87, 497.
   (*b*) *Phy. Rev.*, 1938, **53**, 768.
   (*c*) *Ibid.*, 1938, **54**, 126.
   (*d*) *Quar. Jour. Roy. Met. Soc.*, 1940, Suppl. to Vol. **66**, 41.
   (*e*) *Harvard Met. Studies, No.* **6**, Blue Hill Met. Obs. 1942.
8. The Physical Society .. *Reports on Progress in Physics*, 1943, *Vol.* 9; *Reports of the Gassiot Committee of the Royal Society*.
9. (*a*) Adel .. *Astrophy. Journ.*, 1939, **89**, 1.
   (*b*) Adel and Lampland .. *Ibid.*, 1940, **91**, 1.
   (*c*) ———— .. *Ibid.*, 1940, **91**, 481.
10. Weber and Randall .. *Phy. Rev.*, 1932, **40**, 835 ; 1937, **52**, 160.
11. Martin and Barker .. *Ibid.*, 1932, **41**, 291.
12. Schnaidt .. *Ger. Beitr. z. Geophy.*, 1939, **54**, 203.
13. Callendar .. *Quar. Jour. Roy. Met. Soc.*, 1941, **67**, 263.
14. Strong .. *Jour. Frank. Inst*, 1941, **231**, 121.
15. ———— .. *Ibid.*, 1941, **232**, 1.
16. Abbot .. *Smithsonian Tables*.
17. Edison Pettit .. *Astrophy. Jour.*, 1940, **91**, 159.
18. Meyer .. *Ann. der Phys.*, 1903, **12**, 849.
19. Läuchli .. *Zeit. Physik.*, 1929, **53**, 92.
20. Fabry and Buisson .. *J. Physique*, 1913, (5) 3, 196.
21. Ny and Choong .. (*a*) *C. R. Acad. Sci. Paris*, 1933, **196**, 916.
   (*b*) *Chinese J. of Physics*, 1933, **1**, 38.
22. Chapman .. *Proc. Phy. Soc.*, 1939, **51**, 93.
23. E. Vassy .. Conference on Atmospheric Ozone, *Quar. Jour. Roy. Met. Soc.*, 1936, Suppl. to Vol. **62**, 25.
24. ———— .. (*a*) *C. R. Acad. Sci. Paris*, 1936, **202**, 1426 :
   (*b*) *Ibid.*, 1936, **203**, 1363.

25. E. Vassy .. *Ann. de Phy. Paris*, 1937, **8**, 707.
26. Colange .. *J. Physique*, 1927, (6) **8**, 254.
27. A. Tournaire-Vassy .. *C. R. Acad. Sci. Paris*, 1937, **204**, 1413.
28. Cabannes and Dufay .. *J. de Physique*, 1926, (6) **7**, 257.
28*a*. Fowle .. Cited in **28**.
29. Götz .. *Ergebnisse der Kosmischen Physik*, 1938, **3**, 259.
30. K. Ångström .. *Ark. Matem. Astrom. Phy.*, 1904, **1**, 345 & 395
31. Ladenburg and Lehmann .. *Ann. der Phys.*, 1906, **21**, 305.
32. Gerhard .. *Phy. Rev.*, 1932, **42**, 622.
33. Hettner, Pohlmann and Schumacher .. *Z. Physik*, 1934, **91**, 372.
34. Hertz .. *Verh. Phy. Ges.*, 1911, **13**, 617.
35. Eva von Bahr .. *Ann. der Phys.*, 1909, **29**, 780 ; 1910, **33**, 585.
36. Barker .. *Astrophy. Jour.*, 1922, **55**, 391.
37. Fowle .. *Annals of Astrophy. Obs. Smith. Inst.*, 1922, **4**, 280.
38. Hettner .. *Ann. der Phys.*, 1918, **55**, 476.
39. Fox and Martin .. *Proc. Roy. Soc. A*, 1940, **174**, 234.
40. Penndorf .. *Met. Zeit.*, 1941, **58**, 103 ; *Bull. Am. Met. Soc*., 1944, **25**, 115.
41. Simpson .. *Mem. Roy. Met. Soc. III*, No. 21, 1928.
42. Ramanathan .. *Beitr. z. Phys. der freien Atm.*, 1932, **18**, 196.
43. Brunt and Kapur .. *Quar. Jour. Roy. Met. Soc.*, 1938, **64**, 510.
44. Brunt .. *Ibid.*, 1940, Supp. to Vol. **66**, 34.

SYNTHESIS OF 5: 6-HYDROXY-FLAVONOLS
PART III

By S. Rajagopalan, L. Ramachandra Row and T. R. Seshadri
(*From the Department of Chemistry, Andhra University*)

Received December 29, 1945

In Part II[1] the synthesis and study of 3 : 5 : 6 : 3′ : 4′-pentahydroxy-flavone and its derivatives were described. Following the same procedure the two lower members of this series have now been prepared and their properties studied.

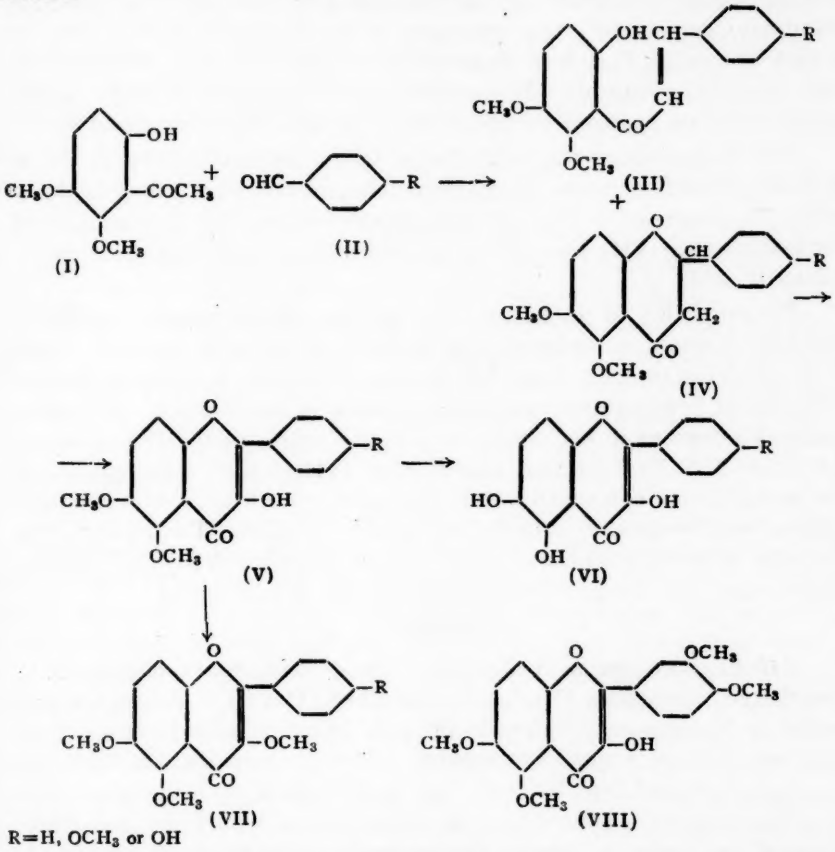

R=H, OCH_3 or OH

Since in the chalkone condensation it is necessary to have the hydroxyl groups protected as far as possible in order to get good yields, 2-hydroxy-

5: 6-dimethoxy-acetophenone (I) was employed instead of the more easily available 2: 5-dihydroxy ketone and the condensation made with benzaldehyde and anisaldehyde. In each case the product was a mixture of both the chalkone and the corresponding flavanone. Similar mixture resulted even when the chalkone was heated with alcoholic sulphuric acid. The conversion of the flavanone into flavonol was effected directly in one stage since it gives better yields of the products.

The 5: 6-hydroxy-flavonols described in the course of this work form a series of compounds lacking a hydroxyl group in the 7-position. There is marked absence of fluorescence as compared with the 7-hydroxy and 5: 7-dihydroxy compounds. The importance of the 7-position for this property is thus indicated. They form brownish-red solutions in alkali which rapidly fade on shaking with air. This characteristic seems to be also due to the presence of two hydroxyl groups in the contiguous positions 5 and 6.

The compounds of type (V) having only a hydroxyl group in the 3-position exhibit fluorescence in alcoholic solutions but not in strong sulphuric acid. They also give prominent ferric chloride colour. The fully methylated compounds (type VII) also give some fluorescence in alcohol but none in sulphuric acid.

The possibility of the flavone ring opening and reclosing in a different direction, during demethylation using boiling hydriodic acid, has been shown to be present in the case of the 5: 8-hydroxy flavones.[3] No definite example is known of 5: 6-hydroxy compounds changing in this manner. This point has been examined in one typical case in the course of the present work. 3-Hydroxy-5: 6: 3′: 4′-tetra-methoxy-flavone (VIII), was demethylated to the pentahydroxy compound which was again remethylated with dimethyl sulphate and potassium carbonate in acetone solution. The product was found to be identical with that of direct methylation of (VIII) thus showing that no isomeric change is involved during the demethylation.

Experimental

2-Hydroxy-5:6-dimethoxy-chalkone :—To a solution of 2-hydroxy-5: 6-dimethoxy-acetophenone (3 g.) and benzaldehyde (5 c.c.) in alcohol (20 c.c.) cooled to 0°, potassium hydroxide (30 g. in 24 c.c. of water) was added in small quantities at a time with shaking. After the addition, the flask was stoppered tight and kept for four days at the laboratory temperature with occasional shaking. The contents were then diluted with water and ether-extracted in order to remove the unreacted aldehyde and then acidified. The product separated in the form of an orange-red liquid which was taken in ether. The ethereal solution was shaken with aqueous sodium bicarbonate

to remove benzoic acid that was also formed during the reaction. On evaporating the ether, a red liquid was obtained which did not solidify even after keeping in the refrigerator for a number of days. The chalkone was soluble in alkali and gave a reddish brown colour with ferric chloride in alcoholic solution. Crystallisation of the product was attempted using benzene, petrol, alcohol and acetone; but in all cases the chalkone was recovered as a liquid. It was therefore directly employed for conversion into the flavanone.

In another experiment, the alkaline solution left after removing the unreacted aldehyde by means of ether, was saturated with carbon dioxide in the hope of obtaining the chalkone in a crystalline condition. A pale brownish yellow solid separated out (0·2 g.). When crystallised from alcohol using animal charcoal, it came out in the form of colourless silky needles melting at 142–44°. It did not depress the melting point of the flavanone obtained from 2-hydroxy-5:6-dimethoxy chalkone. The filtrate from the flavanone on ether-extraction yielded the chalkone in the form of a viscous red liquid.

5:6-*Dimethoxy-flavanone.*—A solution of the above chalkone (2 g.) in 50% aqueous alcohol (100 c.c.) was treated with concentrated sulphuric acid (3 c.c.) and the resulting solution boiled under reflux for 24 hours. On concentrating the solution, the flavanone separated out in the form of pale yellow silky needles. It was filtered and washed with water. The adhering chalkone was removed by macerating the solid with a weak solution of sodium hydroxide. It then crystallised from alcohol (animal charcoal) in the form of colourless silky needles melting at 142–44° (Found: C, 71·9; H, 5·8; $C_{17}H_{16}O_4$ requires C, 71·8; and H, 5·6%).

5:6-*Dimethoxy-3-hydroxy-flavone.*—To a gently boiling solution of 5:6-dimethoxy-flavanone (0·5 g.) in alcohol (40 c.c.) were added alternately amyl nitrite (3 c.c.) and concentrated hydrochloric acid (20 c.c.; d., 1·19) little by little with stirring. After the addition, the contents were left for two hours with occasional shaking. The solution was then diluted with water (150 c.c.) and the solid product filtered and washed with water. It was crystallised twice from alcohol when the flavonol was obtained as rhombic plates, melting at 216°. Yield, 0·15 g. It gave a reddish brown colour with alcoholic ferric chloride. When reduced in alcoholic solution with magnesium and hydrochloric acid an orange-red colour was developed. It was soluble in aqueous alkali to give an yellow solution. An alcoholic solution of the flavonol exhibited green fluorescence. It dissolved in concentrated sulphuric acid to yield a yellow solution without fluorescence (Found: C, 68·5; H, 4·7. $C_{17}H_{14}O_5$ requires C, 68·5; H, 4·7%).

3:5:6-*Trihydroxy-flavone.*—The above dimethoxy flavonol (75 mg.) dissolved in acetic anhydride (3 c.c.) was treated with hydriodic acid (2 c.c.; d., 1·7) with cooling. The solution was refluxed for an hour in an oil-bath kept at 150–55°. After cooling, it was treated with sulphurous acid when a pale yellow crystalline solid separated out. The aqueous solution along with the solid was ether-extracted. On removing ether a pale yellow crystalline solid was obtained. It was crystallised from ethyl acetate when the dihydroxy flavonol came out as stout rectangular rods melting at 183–85°. Yield, 50 mg. It gave a brown ferric chloride colour and exhibited no fluorescence either in concentrated sulphuric acid or in alcoholic solution. It was insoluble in sodium bicarbonate and carbonate solutions but dissolved in aqueous sodium hydroxide to form a brownish red solution; the colour faded slowly to pale yellow, the change being very fast on shaking with air (Found: C, 67·0; H, 3·7; $C_{15}H_{10}O_5$ requires C, 66·7 and H, 3·7%).

3:5:6-*Trimethoxy-flavone.*—To the above dihydroxy flavonol (40 mg.) in anhydrous acetone (20 c.c.) was added anhydrous potassium carbonate (0·5 g.) and dimethyl sulphate (0·2 c.c.) and the mixture refluxed for 20 hours. The solvent was removed and water added when a very pale yellow solid separated. This was filtered, washed with water and crystallised from benzene-petrol mixture when the trimethyl ether came out as stout rhombohedral prisms melting at 130–32°. It gave no ferric chloride colour in alcoholic solution. It exhibited no fluorescence either in alcohol or in sulphuric acid solution (Found: C, 69·4; H, 4·8; $C_{18}H_{16}O_5$ requires C, 69·2; H, 5·1%).

5:6:4′-*Trimethoxy*-3-*hydroxy-flavone.*—This compound was obtained from the corresponding flavanone[2] in one operation as in the previous case.

The colourless solution of the flavanone (0·5 g.) in alcohol (40 c.c.) gradually turned reddish orange on treatment with amyl nitrite (3 c.c.) and concentrated hydrochloric acid (30 c.c.; d., 1·19). After 2 hours, the liquid was diluted to 200 c.c. with water. Pale yellow shining flakes separated out after some hours. They were collected and crystallised twice from alcohol. The flavonol was obtained in the form of pale yellow broad rectangular plates melting at 172–73°. Yield, 0·15 g. It gave bright bluish green fluorescence in alcohol, benzene and ether solutions. With alcoholic ferric chloride a light brown colour was obtained. It was sparingly soluble in cold aqueous sodium hydroxide yielding a very pale yellow solution. In concentrated sulphuric acid it dissolved forming an orange coloured liquid with no fluorescence (Found: C, 65·8; H, 5·1; $C_{18}H_{16}O_6$ requires C, 65·9; and H, 4·9%).

3:5:6:4′-*Tetramethoxy-flavone*.—The trimethoxy flavonol (0·1 g.) was methylated by refluxing it in a solution of anhydrous acetone (50 c.c.) with dimethyl sulphate (0·3 c.c.) and anhydrous potassium carbonate (1 g.) for 8 hours. At the end of the reaction, the potassium salts were filtered and washed with warm acetone. The filtrate was concentrated on the water-bath (2 c.c.) and treated with water (2–3 c.c.). The semi-solid precipitate did not crystallise even ater keeping for a long time in the ice-chest. It was, therefore, extracted with ether and the residue obtained after the removal of ether was crystallised twice from alcohol when it was obtained as colourless rectangular plates melting at 147–48°. It gave no colour with ferric chloride in alcoholic solution. Its solution in alcohol exhibited bluish green fluorescence. However, fluorescence was absent in concentrated sulphuric acid (Found: OCH_3, 36·0; $C_{19}H_{18}O_6$ requires OCH_3, 36·3%).

3:5:6:4′-*Tetrahydroxy-flavone*.—A solution of 5:6:4′-trimethoxy-3-hydroxy-flavone (0·2 g.) in acetic anhydride was treated with hydriodic acid (d., 1·7; 5 c.c. with cooling.) The resulting solution was refluxed on an oil-bath at 150–55° for 2 hours. It was diluted with water and saturated with sulphur dioxide when an orange coloured precipitate was obtained. When crystallised twice from ethyl acetate, the trihydroxy flavonol was obtained in the form of pale yellow microscopic crystals melting at 305° with slight sintering at 294°. Yield, 0·1 g. With alcoholic ferric chloride a dark olive green colour was obtained. It exhibited no fluorescence either in alcoholic or in strong sulphuric acid solution. It was insoluble in aqueous sodium bicarbonate, but dissolved in carbonate solution giving a fairly stable pale yellow colour. In aqueous sodium hydroxide it formed a brownish red solution which faded slowly to pale brownish yellow; the change was very rapid when shaken with air. It did not show marked colour changes in alkaline buffer solutions; in a solution of pH 12·2, it was bright yellow at first, rapidly turning brown; within 4 minutes it was deep brown, after an hour reddish brown and after 24 hours pale reddish brown (Found: C, 62·8; H, 3·8; $C_{15}H_{10}O_6$ requires C, 62·9, and H, 3·5%).

Summary

The synthesis of 3:5:6:3′:4′-pentahydroxy-flavone was already reported. The lower members of this group of 5:6-hydroxy flavonols with one and no hydroxyl group in the side-phenyl nucleus have now been prepared by Kostanecki's method. The characteristic properties are described.

References

1. Row and Seshadri .. *Proc. Ind. Acad. Sci.* (A), 1945, **21**, 130.
2. Balaiah, Row and Seshadri .. *Ibid.*, 1944, **20**, 274.
3. Wesseley and Moser .. *Monatsh*, 1930, **56**, 97.
4. Baker .. *J.C.S.*, 1939, 1922.

EVIDENCE FOR THE EXISTENCE OF THE "EMISSION LAYER" IN THE ATMOSPHERE

By R. Ananthakrishnan, F.A.Sc.

Received December 11, 1945

1. Introduction

The vertical distribution of temperature in the atmosphere is a factor of great importance in determining the processes of weather. Results of upper air soundings all over the world have shown that broadly the atmosphere can be divided into two thermally distinct zones. In the lower zone, known as the *troposphere*, the temperature decreases steadily with height at the rate of approximately 6° C./km. In the upper region, known as the *stratosphere*, the temperature remains constant or increases slightly with height. The surface of separation between the troposphere and the stratosphere is known as the *tropopause*. The tropopause is approximately 18 km. above the ground at the Equator, about 12 km. high in middle latitudes and 8 km. high at the poles. A problem of fundamental importance in Meteorology, which is as yet not completely solved, is to find out a rational physical explanation for the observed distribution of temperature in the atmosphere.

2. Solar and Terrestrial Radiation

In any attempt to answer this question, we have to start from the fundamental fact that the ultimate source of energy for all atmospheric phenomena is the solar radiation intercepted by the earth and its atmosphere. Since the mean temperature of the system (earth + atmosphere) does not show any appreciable change over long intervals of time, it follows that as much energy is sent back to outer space by this system as is received by it.

There is, however, an essential difference in the spectral characteristics of the incoming and outgoing streams of radiant energy. The solar radiation corresponds approximately to black body radiation at a temperature of 6000 °A; practically the entire energy is confined between the wave-length limits $\lambda = 0{\cdot}15\,\mu$ to $\lambda = 4\,\mu$ with peak intensity at $\lambda_m = 0{\cdot}5\,\mu$. As contrasted with this, the energy of terrestrial radiation is spread out over the band of wave-lengths from about $3\,\mu$ to $120\,\mu$ with peak intensity at about $10\,\mu$ to $15\,\mu$, corresponding to black body radiation at a temperature of 200 to 300 °A. We may, therefore, picture the earth and its atmosphere as constituting a system which is continually absorbing short-wave solar radiation and radiating it back into space in the form of long-wave heat radiation.

3. Radiative Equilibrium

If the entire solar energy reaching the outer surface of the earth's atmosphere passes through without any depletion due to reflection and scattering, then every sq. cm. of the earth's surface would receive on the mean during the day and night 0·5 cal./min. Under radiative equilibrium, therefore, the same amount of energy should be radiated out by each square cm. of the earth's surface. Assuming that the surface radiates like a black body, the mean temperature T is given by:

$$\sigma T^4 = 0{\cdot}5 \text{ cal./cm.}^2 \text{ min.}$$

where $\sigma = 5{\cdot}73 \times 10^{-5}$ erg. cm.$^{-2}$ deg.$^{-4}$·sec.$^{-1}$ (Stefan's constant).

This equation when solved for T gives

$$T = 279\ ^\circ\text{A} = +6^\circ\text{ C.} \qquad (1)$$

We know, however, that about 40% of the incoming solar energy is directly returned to space due to reflection, scattering, etc. If it is assumed that the remaining 60% is absorbed at the surface of the earth, then the corresponding equation for radiative equilibrium becomes

$$\sigma T^4 = 0{\cdot}3 \text{ cal./cm.}^2\text{·min.}$$

which gives

$$T = 246\ ^\circ\text{A} = -27^\circ\text{ C.} \qquad (2)$$

The observed mean temperature of the earth's surface is however + 14° C., *i.e.*, it is higher than either of the above values.

4. "Glass House Effect" of the Atmosphere

What is the reason for this high surface temperature of the earth? In order to understand this, we have to consider the assumptions on which the calculations in the preceding section were based. We tacitly assumed that the atmosphere is perfectly transparent to both solar and terrestrial radiation so that the incoming and outgoing streams of radiant energy pass through the atmosphere without any attenuation. We know, however, that while the atmosphere is largely transparent to short-wave solar radiation, it is highly opaque to wave-lengths in the range of terrestrial radiation, because the water vapour and CO_2 always present in the atmosphere possess intense absorption bands in this spectral region. Consequently, the greater part of the heat radiation from the earth's surface is absorbed and trapped by the water vapour and CO_2 in the lowest layers of the atmosphere. These constituents in their turn re-radiate energy over the same wave-lengths at which they absorb, so that a downward stream of radiant energy is directed toward the surface of the earth from the lower layers of the atmosphere (Gegen-

strahlung). The net loss of energy from the surface of the earth (Ausstrahlung) is now less than before; it is equal to the difference between σT^4 and the Gegenstrahlung. Thus the effect of water vapour and CO_2 is to reduce the loss of heat from the surface of the earth or to increase the surface temperature. This is known as the "Glass House Effect" of the atmosphere.

5. Radiative Loss of Heat from the Atmosphere and Albrecht's Emission Layer

With an atmosphere which absorbs and radiates like a black body, the net loss of heat from the earth's surface would be reduced practically to zero, because all the radiation sent out from the earth will be absorbed in the lowermost layers which have practically the same temperature as the earth and would therefore send back an equal amount of radiation towards the earth. However, the water vapour and CO_2 which constitute the major absorbing and radiating constituents of the lower atmosphere do not absorb all wavelengths in the range of terrestrial radiation. As was first shown by Simpson, the absorption spectrum of water vapour in this spectral region can be broadly divided into three categories:—

(1) The spectral band $8\frac{1}{2}\mu$ to 11μ in which water vapour is completely transparent.

(2) The bands 7μ to $8\frac{1}{2}\mu$ and 11μ to 14μ in which water vapour is semi-transparent.

(3) Wave lengths $< 7\mu$ and $> 14\mu$ for which water vapour is so highly opaque that a small amount (according to Simpson 0·3 mm. of precipitable water) is sufficient to absorb completely all radiation.

Out of the total energy σT^4 radiated from the surface of the earth, the entire amount comprised in the spectral band (1) and a portion of the energy in the spectral range (2) are thus directly lost to outer space. It is estimated that out of the 60% incoming solar energy absorbed by the earth and the atmosphere, about 10% only is disposed of in this way. The remaining 50% of long-wave heat radiation returned to space is contributed by the atmosphere.

From which part of the atmosphere does this large amount of heat radiation which is being continually lost to outer space originate? This is a most important problem in the theory of atmospheric heat radiation. We have seen that the principal absorbing and radiating constituents of the lower atmosphere are water vapour and to a lesser extent CO_2. These constituents, however, send out radiation over the same wave-lengths at

which they absorb intensely. If we now picture the atmosphere as being divided into a number of layers each of which contains the optimum quantity of the absorbing constituents to intercept completely the radiation from the layer below it, then, it is easy to see that outward radiation to space can begin only at such a height above which the amount of water vapour and CO_2 present is insufficient to absorb completely all the radiant energy arriving from below.

Simpson assumed that the stratosphere contains enough water vapour to absorb all the radiation coming from the troposphere and that outward radiation to space from the atmosphere originates only from the stratosphere. Later work has, however, shown that Simpson's assumption requires revision.

From a careful study of the absorption and emission spectrum of water vapour, F. Albrecht came to the conclusion that the greater part of the heat radiation sent out into space from the earth's atmosphere has its origin in the upper troposphere and that this radiation passes through the stratosphere without appreciable depletion. According to Albrecht, radiation to outer space from a cloud-free atmosphere is mostly from a layer of about 3 to 4 km. thickness in the upper troposphere, which he designated as the "*Emission Layer*". The radiation from the emission layer is independent of geographical latitude or of the time of the year and is approximately equal to the selective radiation of water vapour and CO_2 at a temperature of $-50°$ C.

The location of the emission layer in the atmosphere is determined by two important considerations, *viz.*,

(1) It contains an optimum amount of water vapour and CO_2 (the constituents that give rise to emission).

(2) The amount of water vapour and CO_2 above the layer is so small that the radiation from the emission layer passes through without appreciable attenuation.

As the emission layer is a region which is losing heat throughout day and night, it is also a part of the atmosphere which is getting continually cooled due to this heat loss.

According to Albrecht's estimates, the emission layer is located at such a height that the water vapour content at its base is approximately 0·1 gm./m^3 and its top ·01 gm./m^3. Consequently, the height of the emission layer varies with the temperature and humidity content of the atmosphere. It has been estimated by Albrecht that when the atmosphere is hot and humid, the emission layer should lie roughly between the levels corresponding to 233 °A and 213 °A; when the atmosphere is comparatively dry, the emission layer should extend from 243 °A to 223 °A.

More recent researches on the absorption spectrum of water vapour have shown that the absorption coefficients given by the earlier workers are far too high and hence would necessitate a much higher value than what Simpson assumed for the critical quantity of precipitable water which constitutes a " black body " for the range of wave-lengths over which water vapour shows marked absorption. Brunt has pointed out that this would not essentially modify the arguments of Simpson and Albrecht although the base of the emission layer would be lower and its thickness more than what was estimated by Albrecht.

6. Emission Layer and Tropopause

According to Albrecht, the top of the emission layer marks the upper limit of the troposphere in polar and temperate latitudes. In the tropics, however, on account of the strong penetrative convection from below, brought about mainly through the agency of water vapour, the tropopause is carried a few kilometres above the top of the emission layer. As a result of this, the temperature of the upper troposphere (above the top of the emission layer and below the tropopause) in the tropics is *lowered* below what it would normally have been as a result of purely radiative processes. Hence, in radiative heat exchange with the lower layers of the stratosphere the upper levels of the tropical troposphere absorb more heat than they radiate out. This is supposed to be the reason (perhaps only one of the reasons) for the sharp inversion at the tropopause and the rapid increase of temperature in the first few kilometres above that in the tropical stratosphere, a feature which is not observed in higher latitudes where the lower stratosphere is practically an isothermal region.

7. Distribution of Heat and Cold Sources in the Atmosphere

While the long-wave outgoing radiation from the atmosphere causes a perpetual cooling of the upper troposphere, practically all the addition of heat resulting from the absorption of short-wave solar radiation takes place essentially at the surface of the earth and in the lower layers near the surface. Thus vertical temperature gradients are set up in the troposphere which give rise to vertical displacements of air masses when the gradients exceed the limits of stability. Consequently, in spite of the continuous loss of heat from the top and addition of heat at the bottom, a dynamical equilibrium with certain limiting temperatures is established.

If we consider the annual mean heat balance of the system (earth + atmosphere), then according to Albrecht's calculations the incoming energy exceeds the outgoing up to latitude $37\frac{1}{2}°$, while at higher latitudes the reverse conditions obtain. As is well known, it is this peculiar latitudinal distri-

bution of incoming and outgoing energy that brings about the general circulation of the atmosphere.

Bjerknes has divided the troposphere into regions where there is a net gain of heat or a net loss of heat. The former are called heat sources and the latter cold sources. The principal cold source in the atmosphere is Albrecht's emission layer which is continually sending out heat energy into outer space. The principal heat source is the lower troposphere in the tropics and the adjoining temperate latitudes which gains a net excess of energy in radiative heat exchange with the earth's surface and also in the form of latent heat of condensation. Besides this, there is a secondary heat source which is the region comprised between the top of Albrecht's emission layer and the tropopause over the tropics and adjoining temperate latitudes. This is a region which is cooled by convection below its radiative equilibrium temperature and as such gets a net excess of heat by radiative exchange with the lower layers of the stratosphere.

8. Seasonal Variation of Heat and Cold Sources over the Northern Hemisphere

If we consider the vertical distribution of heat and cold sources over the northern hemisphere (Fig. 1), there is a striking difference in the conditions which obtain in the summer and in the winter seasons. In the *northern*

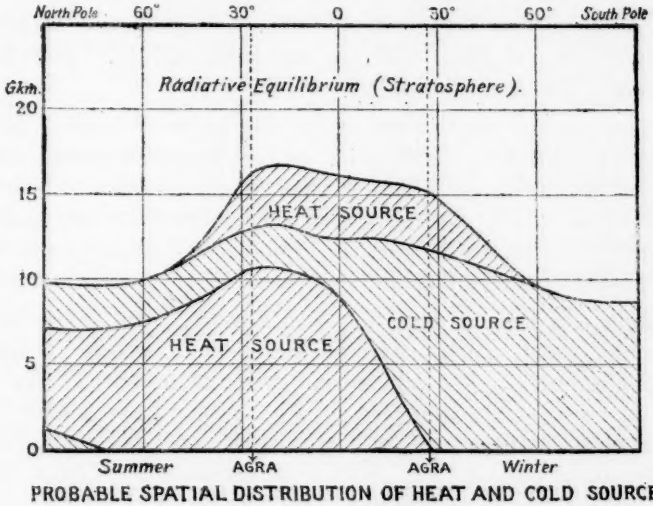

PROBABLE SPATIAL DISTRIBUTION OF HEAT AND COLD SOURCES IN THE ATMOSPHER IN JUNE.

(After Bjerknes)

Fig. 1

summer, practically the whole of the lower troposphere is a heat source; the middle or the upper troposphere (Albrecht's emission layer) forms the cold source. Above this lies the secondary heat source extending from the Equator up to and somewhat beyond 30° N. In the *northern winter*, the lower heat source is displaced towards the southern hemisphere so that the entire troposphere (limited by the top of Albrecht's emission layer) over polar and temperate latitudes is a cold source suffering a continual loss of heat energy. Above the top of this is a feeble heat source which stretches over a part of the temperate latitudes and is in fact an extension of the secondary heat source over the tropics brought about by meridional advection of air.

9. Expected Seasonal Variations in the Thermal Structure of the Atmosphere over Temperate Latitudes Adjoining the Tropics

The considerations of the preceding section would lead us to expect striking seasonal variations in the thermal structure of the atmosphere over a place in the temperate latitudes adjoining the tropics. Such observed variations in their turn can also be regarded as a proof of the general validity of the theoretical considerations outlined in the preceding sections and hence of the existence of the emission layer in the upper troposphere.

What are the changes that we should expect in the thermal structure of the atmosphere over a place such as Agra (lat. 27° 08′: long. 78° 01′) between summer (July) and winter (January)?

Let us first consider the location of the cold source (Albrecht's emission layer) in these two months (see Fig. 1). In July, the atmosphere is hot and humid and the emission layer (following Albrecht) may be taken to be between 11 to 14 gkm. In winter, the entire troposphere below the emission layer is a cold source; the emission layer itself should be between 8 and 11 km. according to the temperate limits given by Albrecht.

In summer, the lower troposphere is a powerful heat source and the condensation of water vapour is by far the most important agency controlling the lapse-rates in the middle and upper troposphere. The lapse-rates at these levels would, therefore, follow the saturation adiabat which, however, is practically parallel to the dry adiabat under the conditions prevailing in the upper troposphere. Within the emission layer itself, there is a continual cooling due to radiation, so that as a result of addition of heat at the bottom and loss of heat from the top there should be a marked tendency for super-adiabatic lapse-rates at these levels. Above the top of the

emission layer, convection and radiation work in opposite directions, the former tending to set up dry adiabatic lapse-rate while the latter tends to establish isothermal conditions. Consequently a rapid decrease of lapse-rate with height should be noticed in the column above the top of the emission layer and below the tropopause. The inversion at the tropopause would be very pronounced and a rapid rise of temperature with height should be the feature in the first few kilometres of the lower stratosphere.

In the winter months, the entire troposphere below the top of the emission layer is a cold source undergoing continual cooling due to radiation. The cooling increases with height and attains a maximum value within the emission layer. The vertical distribution of lapse-rate should thus correspond to what would be expected in an air column which is continually cooled at the top; that is, the highest lapse-rates should occur in and below the emission layer. Above the top of the emission layer, radiative processes alone would set up isothermal conditions. However, meridional movement of air from lower towards higher latitudes transports the characteristics of the tropical tropopause to the temperate latitudes in a less pronounced form. We should thus expect a "composite" type of tropopause over temperate latitudes, the transition from the troposphere to the stratosphere occurring in two stages. The lower transition will correspond to the top of the emission layer, while the upper transition will correspond to the tropopause over the tropics. However, because of the absence of penetrative convection from below, the control by radiation will be more pronounced than in the tropics so that the lapse-rates and upper inversion above the top of the emission layer will be less conspicuous than in the tropics.

In this connection it is interesting to recall a scheme of air circulation between the troposphere and the stratosphere which was suggested by Refsdal some years ago. This is based on the work of Albrecht as well as on the concept originally put forth by Palmén that the tropopause should be regarded as a layer of transition which can dissolve at one level and reappear at a new level in the atmosphere depending upon dynamic as well as radiative conditions. In the temperate latitudes, the tropopause is dynamically sucked down in association with depressions and reforms at its original level when the depression activity has ceased. In this process, therefore, air from the stratosphere is transferred to the troposphere. According to Refsdal, the compensating transport of air from the troposphere to the stratosphere takes place in the tropics where the tropopause is carried above the top of the emission layer by convection, and consequently is constantly striving to build itself at a lower level under the influence of radiation.

From what we have discussed in the preceding, it would appear that the meridional movement of air from lower towards higher latitudes in the upper troposphere furnishes the necessary mechanism for the transport of air from the troposphere to the stratosphere; for, in the absence of penetrative convection from below at the higher latitudes, the high vertical temperature gradients which prevail in the upper levels of the tropical troposphere can no longer be maintained as the air moves over to the higher latitudes. The lapse-rates would, therefore, progressively decrease in the meridionally advancing air column until finally it gets merged with the stratosphere in the higher latitudes. The "composite" tropopause encountered in temperate latitudes appears to mark an intermediate stage in the transition of tropical tropospheric air into stratospheric air of the temperate latitudes.

10. Thermal Structure of the Atmosphere over Agra

A detailed study of the thermal structure of the atmosphere over Agra based on the results of over 500 sounding balloon ascents shows that the observed seasonal variations in the thermal structure of the atmosphere are quite in conformity with what should be expected in the light of Albrecht's work. A detailed account of the investigation is being published elsewhere. Some of the major features brought out by the study might, however, be summarised here:—

(1) In the month of July, the observed lapse-rates in the middle and upper troposphere over Agra practically follow the saturation adiabatic; superadiabatic lapse-rates are frequently encountered between 12 and 14 gkm. Above 14 gkm., the lapse-rate begins to decrease and changes over into an inversion at about 18 gkm.

(2) Following the retreat of the monsoon in September, there is a decrease of lapse-rate in the upper troposphere and an increase in the middle troposphere over Agra.

(3) A sudden decrease of lapse-rate at about 11 gkm. is noticed in a more or less conspicuous form during all the winter months.

(4) The highest lapse-rates in the winter months are noticed between 7 and 11 gkm.

(5) In the winter months, lapse-rates above 11 gkm. are generally feeble and gradually change over to an inversion at about 17 gkm.

(6) The annual range of temperature in the atmosphere over Agra shows two maxima, one at about 9 gkm. and another at about 18 gkm. (see Fig. 2). Starting with the thermal conditions obtaining in summer

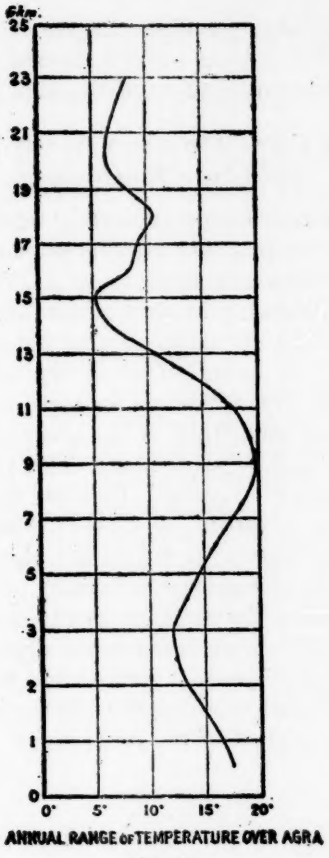

FIG. 2

(July), the lower maximum can be interpreted as the level of maximum cooling in winter (centre of gravity of the emission layer in this season). The upper maximum corresponds to the summer tropopause and is the region where the greatest fall of temperature below that corresponding to radiative equilibrium has been brought about by convection from below. It follows that with decreasing control by convection and increasing control by radiation (transition from the monsoon to winter conditions), there should be a rise of temperature at all levels in the upper troposphere (above the top of the emission layer) and lower stratosphere, the rise of temperature being a maximum at the level of the summer tropopause.

All these facts lend strong evidence for the existence of the "Emission Layer" in the upper troposphere and the seasonal variation of its altitude depending upon the moisture content of the atmosphere.

11. Effect of Ozone Absorption on the Temperature of the Lower Stratosphere

Above the level of the tropopause, vertical transport of heat by convection is not possible, because of the extreme stability of the thermal stratification. Hence the temperature of the lower stratosphere should be conditioned mainly by the balance between absorbed and emitted radiation. In addition to the part played by water vapour and CO_2 at these levels, the absorption and emission by ozone whose average height has been estimated to be between 20 and 25 km. has no doubt to be taken into account in considering the radiative equilibrium of the lower stratosphere. Ozone has a strong absorption band between $0{\cdot}22\,\mu$ and $0{\cdot}33\,\mu$ wherein the incoming solar radiation has appreciable energy. Probably about 5% of the incoming short-wave radiation is absorbed by ozone. Again, ozone has another absorption band in the infra-red at $9{\cdot}5\,\mu$. It is significant that this band is close to the wave-length of maximum energy in terrestrial radiation, while water vapour is transparent for radiation of the same wave-length. A detailed discussion of radiative phenomena in the stratosphere is unfortunately not yet possible because of gaps in our existing knowledge regarding the absorption spectrum of water vapour under stratosphereic conditions as well as of the water vapour content of the stratosphere.

Summary

The theory of radiative equilibrium demands that on the average the total amount of energy absorbed by the earth and its atmosphere in the form of short-wave solar radiation should be exactly equal to the total amount of energy given back to space in the form of long-wave heat radiation. From a study of the absorbing and radiating properties of the atmosphere, F. Albrecht arrived at the fundamental result that the major contribution to the long-wave heat radiation into outer space originates from a layer of some three to four kilometres thickness in the upper troposphere, which he designates as the "*Emission Layer*". The emission layer is thus a portion of the upper atmosphere which is continually cooling due to radiative loss of heat. The height of the emission layer is a function of the water vapour content of the atmosphere; it is more when the atmosphere is hot and humid and less when the atmosphere is cold and dry.

The author has made a detailed study of the thermal structure of the atmosphere over Agra based on the results of sounding balloon ascents over a period of ten years. A number of interesting features find a ready explanation on the assumption that the emission layer over Agra is located approximately between 11 and 14 gkm. in the monsoon months and between 8 and 11 gkm. during the remaining months,—an assumption in conformity with Albrecht's work. The observed seasonal variations in the thermal structure of the atmosphere over Agra thus lend strong evidence for the existence of the emission layer in the atmosphere and the variation of its altitude depending upon the moisture content of the atmosphere.

References

1. G. C. Simpson .. *Mem. Roy. Met. Soc.*, 1928, **3**, No. 21.
2. F. Albrecht .. *Met. Zeit.*, 1931, **48**, 57.
3. V. Bjerknes and others .. *Physikalische Hydrodynamik*, 1933, pp. 663–68.
4. D. Brunt .. *Physical and Dynamical Meteorology*, 1939.
5. ——— .. *Q. J. Roy. Met. Soc.*, 1940, **66**, (Supplement), 34.
6. G. M. B. Dobson .. *Ibid.*, 1942, **68**, 202.
7. A. Refsdal .. *Geophys. Publik.*, 1932, **9**, No. 12.
8. R. Ananthakrishnan .. *On the Thermal Structure of the Atmosphere over Agra* (under publication).

39-46. Printed at The Bangalore Press, Bangalore City, by G. Srinivasa Rao, Superintendent and Published by The Indian Academy of Sciences, Bangalore.